Vesicles formed from phospholipid analogues containing an oligomerisable head group. Properties and mechanism of fusion

Bart Jan Ravoo *† and Jan B. F. N. Engberts *

Physical Organic Chemistry Unit, Stratingh Institute, University of Groningen Nijenborgh 4, 9747 AG, Groningen, The Netherlands. E-mail: j.b.f.n.engberts@chem.rug.nl, bart.ravoo@ucd.ie

Received (in Cambridge, UK) 18th April 2001
First published as an Advance Article on the web 13th September 2001

Covering: 1995–2000

1 Membrane mimetic chemistry
2 Preparation of unilamellar lipid vesicles with oligomerised membrane leaflets [16,18]
2.1 Selective hydrolysis of the β-nitrostyrene group in the outer leaflet of bilayer vesicles
2.2 Photopolymerisation of the β-nitrostyrene group in bilayer vesicles
2.3 Preparation of bilayer vesicles with an oligomerised inner membrane leaflet
3 Properties of vesicles formed from lipids with oligomerisable head groups [16,18,19]
3.1 Differential scanning calorimetry of vesicles of oligomerised lipids [18]
3.2 Lipid monolayer experiments [18]
3.3 ^{31}P-NMR spectroscopy and lipid head group mobility [18]
3.4 Vesicle contents leakage and solubilisation by detergent
4 Calcium-induced fusion of vesicles formed from lipids with oligomerisable head groups [17,19]
4.1 Calcium-induced fusion of vesicles of lipids with β-nitrostyrene head groups
4.2 Asymmetric vesicle fusion
4.3 Fusion of oligomerised bilayer vesicles
5 Electron microscopic investigations of calcium-induced fusion of vesicles with an oligomerised inner membrane leaflet [21]
5.1 Morphology and calcium-induced fusion of vesicles formed from lipid 3
5.2 Calcium-induced fusion of vesicles formed from lipid 1
6 Thermodynamics of calcium-induced vesicle fusion [17]
6.1 Separating calcium ion binding, vesicle aggregation, and bilayer fusion
6.2 Isothermal titration microcalorimetry and the thermodynamics of membrane fusion
7 Fusion of Sendai virus with vesicles of oligomerisable lipids [20]
7.1 Lipid mixing assays and TEM
7.2 Isothermal titration microcalorimetry
8 Conclusions
9 References

1 Membrane mimetic chemistry

The formation of phospholipid bilayer membranes that seclude and compartmentalise all eukaryotic cells is considered to be a prerequisite for the evolution of cell life.[1] Due to the complexity of biological membranes, and due to the lack of powerful *in vivo* analytical techniques, much of our understanding of biological membranes has been derived from experiments using model membranes. Since Bangham's preparation of the first liposomes in 1964,[2] model membrane systems have obtained a degree of sophistication that brings them closer to the level of complexity of *in vivo* membrane functioning. The model membrane system that has found most widespread application is the liposome, a lipid bilayer vesicle enclosing an aqueous compartment. Liposomes can be prepared from a wide range of natural and synthetic lipids and many techniques are available for preparing unilamellar vesicles of a defined size, to enclose water-soluble solutes in the aqueous compartment or to absorb apolar solutes inside the bilayer, and to reconstitute proteins in or at the membrane.[3] Since the discovery of vesicles composed of synthetic amphiphiles,[4] the possibilities for structural variation of lipid and/or amphiphile membrane components has become almost limitless and the field of membrane mimetic chemistry is flourishing.[5–7] Fascinating results have been obtained with giant synthetic liposomes which mimic morphological transformations of the cell[8,9] and with liposomes carrying 'steric shields' of poly(ethylene glycol) which increase colloidal stability and circulation times for medical applications.[10]

All biological membranes are asymmetric. This observation can be rationalised by the fact that each side of the membrane faces a different environment. Almost all membrane-associated proteins and most lipid components are distributed with a high or even absolute transverse asymmetry.[11] A striking example is the membrane of the human erythrocyte which contains at least four asymmetrically distributed lipids: 75% of phosphatidylcholine and 85% of sphingomyeline are located in the outer membrane leaflet, and 80% of phosphatidylethanolamine and over 95% of phosphatidylserine are located in the inner membrane leaflet.[12] The origin and maintenance of biological membrane asymmetry is a complex phenomenon that is far from understood. Artificial asymmetric bilayer membranes provide interesting test models, but apart from the pioneering work of Moss[13] and Ringsdorf[14,15] and co-workers, the properties of such membranes remain largely unexplored.

Here we review our work on a family of synthetic lipid molecules that we used as a tool for providing structural, kinetic and thermodynamic information on properties of lipid bilayers in general and membrane fusion in particular.[16–21] These lipids are phospholipid analogues containing a bifunctional β-nitrostyrene (BNS) unit linked to the phosphate head group (Fig. 1). The BNS head groups of these lipids form linear oligomers upon UV irradiation but hydrolyse under alkaline conditions.[16,18] A kinetic model for surface-specific reactions of vesicular bilayers was developed.[16] Following selective hydrolysis of the BNS groups in the outer membrane

† Present address: Department of Chemistry, National University of Ireland, University College Dublin, Belfield, Dublin 4, Ireland

DOI: 10.1039/b101370j

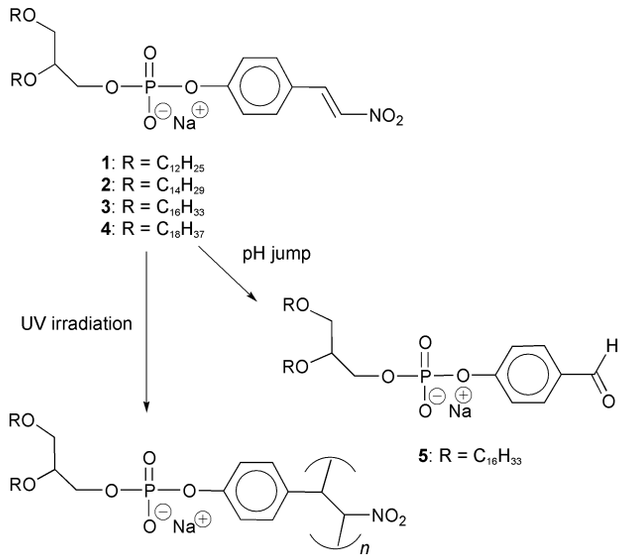

Fig. 1 Molecular structures of the β-nitrostyrene lipids **1**–**4** and the products that result from alkaline hydrolysis and photopolymerisation.

leaflet, the BNS groups in the inner leaflet can be photopolymerised, yielding vesicles with an oligomerised inner leaflet.[16] Vesicles of BNS lipids undergo efficient calcium-induced fusion.[19,21] After oligomerisation of the lipid head groups, the vesicles aggregate upon addition of calcium ion, but calcium-induced fusion is strongly inhibited.[19] Since bilayer vesicles of BNS lipids can be oligomerised exclusively in their inner leaflet, we had access to membranes with an extreme transverse asymmetry: while the outer leaflet is prone to fusion, the inner leaflet is not. Part of our work stems from the assumption that the oligomerisable lipid vesicles present a promising avenue towards structural characterisation of intermediate structures of calcium-induced membrane fusion.[19]

The membrane model system of BNS lipids was further exploited in a microcalorimetric analysis of membrane fusion. There is still only very limited literature on the use of isothermal titration microcalorimetry to investigate the thermodynamics of membrane fusion.[22,23] We used the BNS lipid vesicles to determine the enthalpies associated with the consecutive elementary stages of binding of calcium ion, vesicle aggregation, and bilayer fusion in the course of calcium-induced vesicle fusion.[17] It was found that fusion of small vesicles is associated with a small positive enthalpy and requires a dominant entropic driving force. Furthermore, the fusion of vesicles of BNS lipids with Sendai virus was investigated.[21] It was observed that vesicle–virus fusion is strongly inhibited by lipid head group oligomerisation. According to a microcalorimetric analysis, vesicle–virus fusion is associated with a much larger positive enthalpy than vesicle–vesicle fusion.

In this review we aim to present a critical evaluation of the insights into the properties of bilayer membrane vesicles in general and membrane fusion in particular that we obtained from our model system using oligomerisable lipids. The results are reviewed in the context of the state of the art of membrane mimetic chemistry and current understanding of biological membrane fusion. However, we admit that this review is biased towards our own contributions in this area, and we refer the reader to literature reviews for full coverage of the fascinating topics of membrane mimetic chemistry[6,7] and biological membrane fusion.[24]

2 Preparation of unilamellar lipid vesicles with oligomerised membrane leaflets[16,18]

Central to the development of the model membrane system was the synthesis of a novel class of synthetic phospholipids containing a bifunctional β-nitrostyrene (BNS) unit, and the preparation of small unilamellar vesicles of these lipids. The BNS unit is covalently attached to the phosphate head group and therefore resides at the surface of the bilayer vesicle, partitioned between the inner membrane leaflet (*endo*-surface) and the outer membrane leaflet (*exo*-surface). Surface differentiation of the vesicles was obtained by two simple reactions of the BNS units. On the one hand, BNS derivatives are polymerisable—there is literature describing dimerisation as well as polymerisation of BNS.[25] On the other hand, BNS hydrolyses in alkaline aqueous solution.[26] The hydrolysis involves rate-determining nucleophilic attack by hydroxide ion at the α position of the styrene, leading to an intermediate that rapidly splits into a benzaldehyde and the anion of nitromethane. Both the hydrolysis and the polymerisation reaction can be conveniently monitored using UV-VIS spectroscopy, indicating the disappearance of the absorption of BNS at 335 nm ($\varepsilon = 10^4$ M^{-1} cm^{-1}).

Surface discrimination of reactions at a vesicle surface critically depends on a negligible permeation of reactant(s) through the bilayer and a slow rate of translocation of lipid molecules over the bilayer (flip–flop). These parameters are primarily governed by the thickness of the membrane and the thermotropic state of the membrane interior, which in turn depend on the length of the hydrocarbon chains, and the temperature. In this study, lipids with *n*-dodecyl, *n*-tetradecyl, *n*-hexadecyl and *n*-octadecyl chains were examined (Fig. 1). Since the cleavage reaction occurs in alkaline solution, non-hydrolysable 1,2-di-*n*-alkoxypropanols rather than 1,2-di-*n*-acyloxypropanols were used. The ether linkages make these lipids more robust against pH changes than the naturally abundant esters, without affecting other membrane properties. The product of hydrolysis of the BNS group in lipid **3** is lipid **5**, which was also synthesised independently.

Vesicle solutions were prepared by dispersion of lipids **1**–**5** in water or aqueous buffers (pH 7.4) using a sonication immersion tip. Quasi-elastic light scattering (QELS) revealed number-weighted averages of 50–100 nm for the diameter of vesicles of all lipids. These average diameters were confirmed using transmission electron microscopy (TEM). Alternatively, monodisperse, large unilamellar vesicles were prepared by repeated extrusion through polycarbonate membranes and polydisperse, large multilamellar vesicles were prepared by rapid stirring. In water, all vesicle solutions are stable for at least one week. Vesicle solutions of **1** and **2** in buffers of physiological ionic strength are stable colloids for many days, whereas solutions of **3** and **4** tend to flocculate after about 1 day at room temperature.

The L_β–L_α phase transition temperature (T_m) for each lipid was measured by differential scanning calorimetry (DSC) and characterised by the temperature and enthalpy of transition (Table 1), as well as the patch number *n* and the number of van't Hoff phase transitions (*m*) required to fit to the experimental data, which are a measure for the co-operativity of the phase transition.[27] The relation between T_m and the chain length compares well with the chain length dependence of T_m of phosphatidylcholines and phosphatidylserines reported in the literature.[28] The values of T_m for the BNS lipids are similar to those of phosphatidylcholine with identical chain length and *ca.* 13 °C lower than those reported for phosphatidylserine with identical chain length. Apparently, the bilayer packing efficiency of the BNS lipid molecules is comparable to that of phosphatidylcholines with identical chain length.

2.1 Selective hydrolysis of the β-nitrostyrene group in the outer leaflet of bilayer vesicles

Hydrolysis of the BNS units at the vesicle surface was initiated by dilution of a small volume of a solution of vesicles prepared at pH 7.4 into a solution of pH 11.5. Alternatively, a small volume of NaOH solution of known concentration was added

Table 1 Differential scanning calorimetry of vesicles of **1**–**5** in water

	Small vesicles (sonication)				Large vesicles (stirring)			
Lipid	T_m/°C	Enthalpy/kJ mol^{-1}	*n*	*m*	T_m/°C	Enthalpy/kJ mol^{-1}	*n*	*m*
1	nd	—	—	—	−1	25.0	nd	—
2	nd	—	—	—	21.6	28.5	143[a]	11[a]
3	39.9	29.8	154	7	40.7	42.3	121	4
4	52.0	21.6	200	6	53.8	37.8	201	5
5	37.6	21.7	268	7	40.4	44.6	139	5

[a] Includes secondary transitions around 40 °C.

to a sample of vesicles, raising the external pH from 7.4 to 11.5. In either way, vesicles with neutral internal pH and high external pH were obtained. Surface differentiation now critically depends on the ratio between the rate of BNS hydrolysis and the permeability of the bilayer to hydroxide ion (or protons) as well as the rate of exchange of lipid molecules between the two membrane leaflets (flip–flop). Hydroxide ion/proton permeation through the bilayer (at room temperature) depends on the length of the hydrocarbon chains. We demonstrated that the pH gradient is maintained during the cleavage experiments using vesicles of **3**, and that hydroxide ion (or proton) permeation is negligible.[18] For lipid **1**, at temperatures above T_m, hydroxide leakage is considerable. Similar observations were made for the bilayer permeation of carboxyfluorescein (*vide infra*). Secondly, surface differentiation is favoured by an increase of the length of the alkyl chains and by low temperatures ($T < T_m$), because flip–flop is retarded by these factors.[29,30]

In a first approximation, the hydrolysis was analysed in terms of a model in which it is assumed that the BNS units are partitioned between the outer or *exo*-vesicular and inner or *endo*-vesicular surfaces of the vesicles. The *exo*-vesicular part of the BNS groups is easily accessible to nucleophilic attack by hydroxide ion and will undergo a relatively rapid hydrolysis characterised by k_{fast}. On the other hand, the *endo*-BNS groups are much less accessible (since prior to cleavage they will have to translocate over the membrane) and will undergo a much slower hydrolysis characterised by k_{slow}. UV-VIS spectroscopy does not discriminate between $[BNS]_{exo}$ and $[BNS]_{endo}$, and so the decrease of $[BNS]_{exo\,+\,endo}$ with time is monitored. The decrease of this concentration was fitted to a double pseudo-first-order rate equation with $k' = k[OH^-]$ to give eqn. (1).

$$[BNS]_{exo\,+\,endo} = [BNS]_{exo,0}\exp(-k'_{fast}t) + [BNS]_{endo,0}\exp(-k'_{slow}t) \quad (1)$$

The model was then extended to include flip–flop of lipid molecules (Fig. 2). With lipid flip–flop characterised by k_1 and k_{-1} and *exo*-vesicular hydrolysis of BNS by $k'_2 = k_2[OH^-]$ to give eqn. (2) and (3).

$$d[BNS]_{endo}/dt = -k_1[BNS]_{endo} + k_{-1}[BNS]_{exo} \quad (2)$$

$$d[BNS]_{exo}/dt = k_1[BNS]_{endo} - k_{-1}[BNS]_{exo} - k'_2[BNS]_{exo} \quad (3)$$

This leads to an equation of the form given in eqn. (4).

$$[BNS]_{endo\,+\,exo,t} = C_a\exp(-k'_{slow}t) + C_b\exp(-k'_{fast}t) \quad (4)$$

The solution for $[BNS]_{endo\,+\,exo,t}$ was found using Laplace transforms.[16] C_a, C_b, k'_{slow} and k'_{fast} are combinations of $[BNS]_{exo,0}$, $[BNS]_{endo,0}$, k_1, k_{-1} and k'_2. Thus, assuming k_1 equals k_{-1} (lipid molecules flip and flop at equal rate), k_1 and k'_2 and also $[BNS]_{exo,0}$ and $[BNS]_{endo,0}$ may be calculated from the experimentally determined values of k'_{slow} and k'_{fast}. Whereas k'_2 is similar for all BNS derivatives, there is a clear trend in k_1. *endo*-Vesicular cleavage is most significant in the vesicles of the lipids with the shortest alkyl chain (**1** and **2**), in which most rapid flip–flop is anticipated.[29,30] At 25 °C, surface differentiation is impossible in vesicles of **1** (k_1 equals k'_2) and problematic in vesicles of **2** (k_1 is not much smaller than k'_2). On the other hand, in vesicles of **3** and **4**, k_1 is small relative to k'_2. Surface differentiation is easily achieved and can be maintained over periods of several hours. The half-life of flip–flop in vesicles of **3** is more than six hours. These rates of flip–flop are similar to those reported for comparable model systems.[13] The BNS persisting in vesicles of **3** and **4** after more than 4 half-lives of the *exo*-vesicular hydrolysis is unreacted *endo*-BNS. The relative amounts of *exo*-BNS and *endo*-BNS match expectations from calculations for small vesicles. At temperatures above T_m, k_1 approaches k'_2 and the cleavage reaction follows first-order kinetics. Most likely, this result is due to faster flip–flop above T_m. Also, above T_m considerable hydroxide leakage is expected.

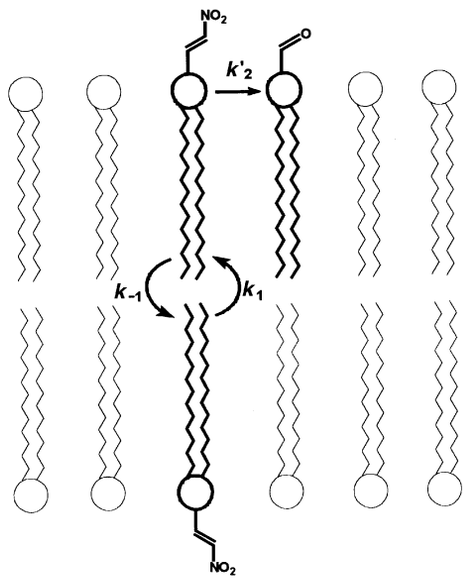

Fig. 2 Kinetic model for the surface-specific hydrolysis of the β-nitrostyrene moiety and lipid flip–flop in bilayer vesicles. (Top: *exo*- or outer membrane leaflet, bottom: *endo*- or inner membrane leaflet.) Lipid structures have been simplified for clarity.

Fig. 3 presents the hydrolysis of the BNS moieties in vesicles of lipid **3** under various experimental conditions, and illustrates the approach to surface-differentiated vesicles. At 25 °C, the *exo*-vesicular BNS groups are hydrolysed with a half-life of *ca.* 25 min ($k'_2 = 5.13 \times 10^{-4}$ s^{-1}), but the *endo*-vesicular BNS groups remain unaffected for several hours because only slow flip–flop occurs ($k_1 = 3.43 \times 10^{-6}$ s^{-1}) and the pH gradient is maintained. When cetyltrimethylammonium bromide (CTAB) is added, the vesicles are solubilised and the remaining BNS groups hydrolyse rapidly with CTAB micellar catalysis. If the reaction is carried out at 46 °C, both flip–flop and leakage are rapid, and all BNS groups react equally fast ($k'_2 = 2.14 \times 10^{-3}$ s^{-1}).

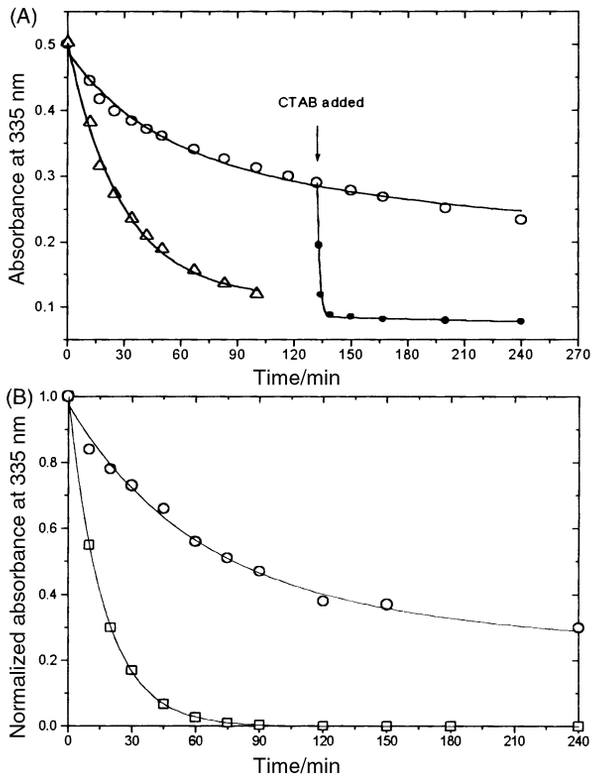

Fig. 3 (A) Decrease of BNS absorbance with time during hydrolysis of vesicles of lipid **3** at pH 11.5. ○: Selective *exo*-vesicular hydrolysis at 25 °C. △: Non-selective hydrolysis at 50 °C. ●: Solubilisation of the vesicles by CTAB after two hours of selective *exo*-vesicular hydrolysis at 25 °C, and fast hydrolysis of the remaining *endo*-vesicular BNS groups. (B) Hydrolysis of BNS groups of vesicles of lipid **1**. The absorbance has been normalised. ○: Selective *exo*-vesicular hydrolysis at 5 °C and pH 12. □: Non-selective hydrolysis at 25 °C and pH 11.5.

Fig. 3 also presents data for the hydrolysis of the BNS moieties in vesicles of lipid **1** at room temperature and at 5 °C. At room temperature and pH 11.5, hydroxide/proton leakage and lipid flip–flop are rapid, and *exo* and *endo*-vesicular BNS groups hydrolyse equally fast ($k' = 1.0 \times 10^{-3}$ s^{-1}). However, when the hydrolysis is performed at 5 °C and pH 12 (the hydrolysis is too slow at pH 11.5), a reasonable degree of surface discrimination can be achieved because the rates of leakage and flip–flop are reduced. A double exponential fit to the decrease of $[BNS]_{endo + exo}$ with time yields the rate of *exo*-vesicular hydrolysis $k'_2 = 3.4 \times 10^{-4}$ s^{-1} and the rate of flip–flop $k_1 = 9.0 \times 10^{-5}$ s^{-1}. The ratio k'_2/k_1 equals 4 and surface discrimination is possible provided the vesicles are kept at *low* temperature.

QELS and TEM showed that sonicated vesicles of lipid **5**, the product of the hydrolysis of **3**, have similar size as vesicles of **3**. The DSC enthalpogram of large vesicles of **5** is almost identical to that of **3**. Evidently, the hydrolysis influences neither the vesicle size nor the thermotropic behaviour of the bilayer.

2.2 Photopolymerisation of the β-nitrostyrene group in bilayer vesicles

Rapid photopolymerisation of the BNS moiety was achieved by UV irradiation.[16,18] No initiator was required. No monomer could be detected by UV-VIS spectroscopy after irradiation for 10 min (Fig. 4). Polymerisation of β-nitrostyrene in solution is difficult,[25] but it is known that polymerisation reactions benefit entropically from the close proximity of the monomers in the bilayer.[31,32] Polymerisation of BNS in vesicles also takes place under influence of sunlight and heating,[33] whereas the pure lipids or lipid stock solutions are stable. Therefore, vesicle solutions were always protected from sunlight and prolonged

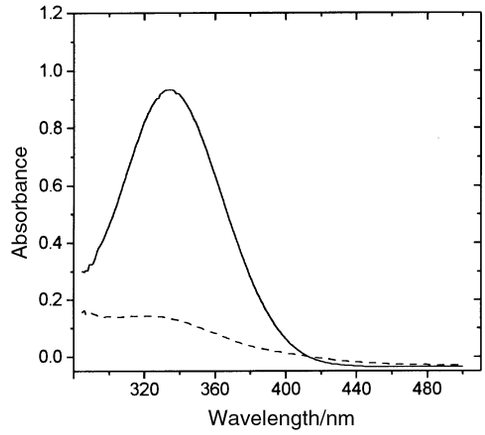

Fig. 4 Disappearance of the absorbance of the β-nitrostyrene moiety after photopolymerisation of vesicles formed from lipid **1** for 10 min. The solid line represents the absorbance before polymerisation, the dashed line after polymerisation.

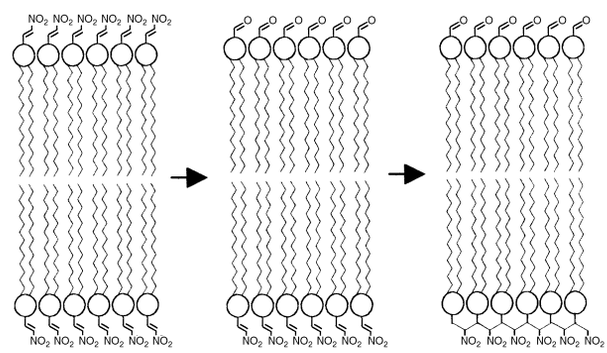

Fig. 5 Illustration of the protocol to obtain vesicles with an oligomerised inner bilayer leaflet. Lipid structures have been simplified for clarity.

heating. QELS and TEM showed that the average size and integrity of the vesicles were unaffected by the polymerisation.

Characterisation of a lipid polymer is troublesome due to its amphiphilic nature and is usually accomplished after removal of the hydrophobic moiety by hydrolysis or transesterification.[34–37] However, lipids **1**–**4** are alkyl ethers, and also the phosphodiester is surprisingly stable to hydrolysis. Gel permeation chromatography of polymerised **1** was not successful. No cyclobutane-like dimers[25] could be detected in the electrospray mass spectrum of polymerised **1**. Vapour pressure osmometry yielded an average molecular weight (M_n) for polymerised **1** of 2470, corresponding to an average polymerisation degree of 3.8. Unfortunately, this technique is time-consuming and demands large amounts of material for each analysis. In addition, since osmometry is extremely sensitive to the presence of low-molecular weight impurities (such as water and salts) the molecular weight should be considered a low estimate. For these reasons, no extensive study of the influence of temperature, concentration, addition of initiator, irradiation time, *etc.* on the polymerisation was carried out. It was concluded that 10 min of intense UV irradiation of vesicles of BNS lipids at room temperature results in formation of oligomers rather than long polymers.

2.3 Preparation of bilayer vesicles with an oligomerised inner membrane leaflet

Combination of selective *exo*-vesicular hydrolysis and *endo*-vesicular oligomerisation of the BNS lipids presents a simple method for preparing vesicles with an asymmetric bilayer (Fig. 5). Vesicles of **3** and **4** were exposed to an external pH of 11.5 at room temperature for a period of *ca.* 1.5 h, after which

exo-vesicular hydrolysis of BNS is complete. Subsequently, the vesicle solution was neutralised and irradiated with UV light for 10 min. In this way, vesicles containing an oligomerised inner membrane leaflet and a monomer outer membrane leaflet were obtained. According to QELS and TEM, neither the *exo*-vesicular hydrolysis, nor the *endo*-vesicular oligomerisation had significantly affected the average size and integrity of the vesicles (*vide infra*). Presumably, the degree of oligomerisation of the inner membrane leaflet is similar to that for vesicles in which both leaflets were oligomerised. Thus, vesicles were obtained which contain an oligomerised inner membrane leaflet and a monomer outer membrane leaflet. To the best of our knowledge, these vesicles represent the first examples of bilayers that are polymerised exclusively in one of the two membrane leaflets. Only vesicles in which the counterions were polymerised in a surface-specific manner have been described previously.[14]

3 Properties of vesicles formed from lipids with oligomerisable head groups[16,18,19]

Since the early 1980's, a large variety of lipids that can be polymerised within the bilayer has been synthesised.[15,35,38,39] Polymerisable groups have been introduced at either end and in the middle of the hydrophobic chains of lipids, as well as in the hydrophilic head groups, and even in the counterions of ionic lipids.[14,40,41]

Photopolymerisations are known as well as chemically-initiated polymerisations. The kinetics and degree of polymerisation have been examined in detail for several polymerisable lipids.[31,36,42] Depending on the structure of the polymerisable lipid, and particularly the position of the polymerisable unit, the effect of polymerisation on the bilayer can be very different. Roughly speaking, polymerisable lipids can be divided into two classes: a large group of lipids for which the bilayer is *stabilised* upon polymerisation, and a small group of lipids for which the bilayer is *destablised* upon polymerisation. Polymerisable lipids of the first type are of interest for therapeutic applications because covalent linking of the lipid molecules yields liposomes with a higher colloidal, physical and chemical stability. Furthermore, liposomes of polymerised lipids retain their aqueous contents much longer than their monomer lipid counterparts.[35] Polymerisable lipids of the second kind are often unstable because the polymerised lipid tends to adopt a non-bilayer structure which leads to leakage of the liposome contents and (in some cases) liposome aggregation and fusion.[43,44] This destabilisation opens challenging possibilities for photo-induced liposomal contents release and/or fusion.

3.1 Differential scanning calorimetry of vesicles of oligomerised lipids[18]

The changes in thermotropic behaviour of bilayers upon lipid polymerisation are highly dependent on the molecular structure of the lipid and the location of the polymerisable unit.[45] Polymerisation of hydrocarbon chains generally leads to a loss of a well-defined main phase transition, whereas polymerisation of head groups leads to increased head group packing without significantly affecting hydrocarbon chain flexibility. Polymerisation of counterions influences the packing efficiency by its drastic effect on the hydration of head groups.

Bilayers of lipids **1**–**5** have main phase transition temperatures (T_m) similar to those of phosphatidylcholines, but much lower than those for phosphatidylserines with identical chain lengths. Upon oligomerisation of the lipids, different thermotropic behaviour is found. Although only a marginal shift of T_m was observed upon oligomerisation, a pronounced 'shoulder' (extending over 10–15 °C) develops at the high temperature side of the main peak in the enthalpogram. The overall enthalpy of the phase transition(s) is unaffected, but the number of van't Hoff phase transitions (m) required to fit to the experimental data increases and the patch number n decreases upon oligomerisation. If only the inner membrane leaflet is oligomerised, the results are similar but the 'shoulder' is less pronounced. Hydrolysis of the BNS group has no detectable influence on the thermotropic behaviour of the lipid bilayer.

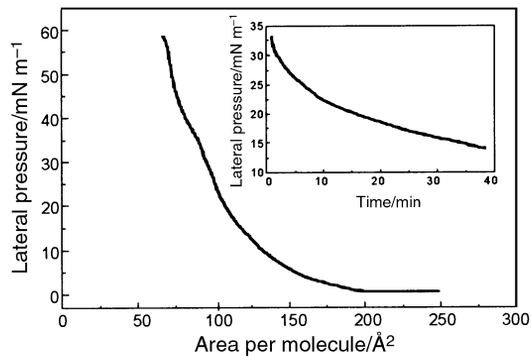

Fig. 6 Lateral pressure *versus* molecular area curve for compression of a monolayer of lipid **3** on the air–water interface. Insert: decrease of lateral pressure with time during UV irradiation of a monolayer of **3** at moderate compression.

In sum, oligomerisation of the BNS groups has two distinct effects on the bilayer melting behaviour. Firstly, a modest but significant part of the lipid melts at higher temperature. This indicates that there is a portion of the lipid material in which the lipid molecules are packed more efficiently after oligomerisation. Since oligomerisation occurs in the lipid head group rather than in the hydrocarbon chains, the increased lipid packing is not a result of a reduced mobility of the hydrocarbon chains. Most likely, the lipid packing efficiency increases because the head group packing becomes more efficient upon oligomerisation, both as a direct consequence of the covalent linking of the BNS groups, and indirectly because oligomerisation of the head groups could entail a loss of some hydration water. We suggest that oligomers of BNS lipids have a lipid packing efficiency (and T_m) more similar to that of phosphatidylserines rather than that of phosphatidylcholines because the lipid head group interaction is more favourable in bilayers of the oligomers than in bilayers of the monomers. However, most of the lipid still undergoes the main phase transition at the same temperature. Perhaps the shoulder only reflects the packing in the largest oligomers, and not in the short ones. Secondly, the co-operativity of melting decreases, as anticipated on going from a homogeneous bilayer of identical lipids to disperse mixtures of oligomers, and a completely asymmetric membrane in the case where only the inner membrane leaflet is oligomerised. This decrease in co-operativity has been reported for comparable lipid head group polymerisations.[46,47] The constant enthalpy of transition reflects the fact that an identical number of identical hydrocarbons undergoes the same phase transition.

3.2 Lipid monolayer experiments[18]

Studies of lipid monolayers on the air–water interface provide valuable insight into the molecular surface area, the thermotropic behaviour and the miscibility of lipids in bilayer membranes.[48] Polymerisation of lipid molecules may affect all these properties.[15,49] Preliminary experiments were carried out with lipid **3** at room temperature (Fig. 6). This lipid spreads readily on the air–water interface, and the area–pressure curve at 20 °C shows a minimal molecular surface area of 65 Å^2 and a collapse pressure of about 60 mN m^{-1}. The molecular surface area is rather high for a monolayer of lipids with two saturated hydrocarbon chains (it is *ca.* 45 Å^2 for phosphatidylcholines),[48] which could indicate that the hydrophobic BNS head groups partly fold back into the lipid monolayer and obstruct a regular monolayer packing. Upon UV-irradiation of the monolayer

at moderate compression (30 mN m^{-1}) and constant area, a gradual decrease in the pressure–time diagram is observed. This decrease in pressure probably reflects partial collapse of the monolayer as a result of increasing packing stress in the course of the oligomerisation reaction. The surface pressure is relieved because the monolayer (partially) becomes a bi- or multilayer. One might also argue that the packing of the lipid oligomers that are formed is more compact than the loose assembly of monomers at 30 mN m^{-1} compression, and that contraction of the lipid head groups due to oligomerisation leads to curvature stress in the monolayer.[32] The pressure–time curve of the monolayer under UV-irradiation (Fig. 6, insert) was used to estimate the kinetics of the photopolymerisation. Photopolymerisation of the monolayer at ambient temperature proceeds with a half-life of about 10 min. It should be noted that the intensity of the UV source used in the monolayer experiment was much lower than that routinely used for photopolymerisation of bilayer vesicles. The kinetics of oligomerisation need not be the same in both systems.

3.3 ^{31}P-NMR spectroscopy and lipid head group mobility[18]

^{31}P-NMR spectra of small unilamellar vesicles of lipid **1** yielded insight into the effect of oligomerisation on the head group mobility of the lipids in the bilayer. Prior to oligomerisation, the spectrum shows an isotropic signal with a line width of *ca.* 30 Hz. This signal is indicative of small vesicles that tumble fast and of rapid lipid lateral diffusion within the vesicle bilayer.[50] After photopolymerisation of the same vesicle solution, a line width of *ca.* 230 Hz was found. Since slower tumbling of oligomerised lipid vesicles relative to monomer lipid vesicles can be excluded because no significant change of vesicle diameter was observed upon oligomerisation, the eight-fold increase in line width indicates slower lateral diffusion of the lipid oligomers in the bilayer. (However, a contributing line-broadening due to chemical shift differences between the polydisperse oligomers cannot be excluded.) Slower lateral diffusion was also observed in a study of the influence of head group polymerisation on the molecular mobility of synthetic cationic lipids.[51] For comparison, a five-fold *decrease* in ^{31}P line width was reported for small unilamellar vesicles of dipalmitoyl phosphatidylcholine upon an increase in temperature from 30 to 50 °C, *i.e.* from below to above the main phase transition temperature.[32] By means of a viscosity dependence study of the line width, this decrease in line width was correlated with a twenty-fold increase of the lateral diffusion coefficient of the lipid molecules.[32] These NMR data indicate that oligomerisation results in a large decrease of lateral diffusion. For most lipids in a liquid-crystalline bilayer, the lateral diffusion coefficient (D_{lat}) is about 1 μm^2 s^{-1}.[12] The mean square lateral displacement of a lipid molecule in time t is given by $4D_{lat}t$. If we assume that the reduction of the diffusion coefficient upon oligomerisation of **1** is *at least* twenty-fold, then while the lipid monomer would take 25 ms to travel around a vesicle with a diameter of 100 nm, the lipid oligomers would need more than 500 ms.

3.4 Vesicle contents leakage and solubilisation by detergent

A straightforward method for measuring the permeability of bilayer membranes involves encapsulation of a fluorescent solute at self-quenching concentration in the aqueous interior of unilamellar vesicles.[3] After removal of non-encapsulated solute by gel permeation chromatography, the leakage of the entrapped fluorescent solute results in high dilution, with concomitant relief of self-quenching and increase of fluorescence intensity. The contents leakage of small vesicles of lipids **1** and **3** was monitored by measuring the release of entrapped carboxyfluorescein (CF). The encapsulation efficiency for both types of lipid vesicles measured using UV-VIS spectroscopy is 8–12 nmol CF per μmol of lipid. This efficiency is normal for small unilamellar vesicles.[3] Release of entrapped CF is strongly dependent on the lipid, lipid oligomerisation, and temperature. For **1**, the vesicles are rather leaky at room temperature. The half-life of contents release is 10 min. Upon oligomerisation of **1** in both membrane leaflets of the vesicles, the vesicles retain their contents much longer—for oligomerised **1**, the half-life of release is one hour. Compared to **1**, vesicles of **3** are not leaky. At room temperature, less than 3% of entrapped CF is lost from the vesicles after two days, irrespective of whether the lipids have been oligomerised or not. However, at 50 °C ($T > T_m$) vesicles of **3** are permeable to CF. Prior to oligomerisation, most of the entrapped CF is released within 15 min. If both membrane leaflets are oligomerised, the bilayer is much less permeable. The half-life of contents release increases to more than two hours. If only the inner membrane leaflet is oligomerised, the vesicles are only slightly more permeable. Hence, the inner membrane leaflet poses the primary barrier for outward permeation. The initial rate of solubilisation of small unilamellar vesicles of **3** by the nonionic detergent Triton X-100 was measured as the initial rate of relief of self-quenching of *n*-octadecyl rhodamine upon addition of the detergent to the vesicle solution. Solubilisation is slower by a factor of two for the oligomerised bilayer relative to the monomer lipid bilayer, irrespective of whether only the inner or both membrane leaflets are oligomerised. Possibly, the process of bilayer swelling due to uptake of detergent, which is considered to be the first step in solubilisation by nonionic detergents,[53] proceeds less readily in oligomerised bilayers than in monomer bilayers, irrespective of whether the oligomers are present in both membrane leaflets, or only in the inner one. In conclusion, compared to their monomer lipid counterparts, the oligomerised lipid vesicles are less permeable and more resistant towards detergent solubilisation. Oligomerisation can be considered a mild form of polymerisation, for which similar observations are reported: generally, vesicles of polymerised lipids retain their contents longer and have a higher stability towards solubilisation by detergents and alcohols.[35] Permeability and detergent solubilisation are affected to an equally large extent when either both or only the inner membrane leaflet is oligomerised.

4 Calcium-induced fusion of vesicles formed from lipids with oligomerisable head groups[17,19]

If the formation of phospholipid bilayer membranes which seclude and compartmentalise all eukaryotic cells was a prerequisite for the evolution of cell life, then transport over the membrane is a primordial mode of communication between the various compartments in the cell, as well as with the extracellular world. Along with translocation mediated by proteins and ionophores,[12] membrane fusion provides the main gateway across the bilayer membrane for a myriad of compounds. Whereas ionophores and the channels formed by proteins generally provide exclusive entry or exit pathways for a small solute such as an ion or a molecule, membrane fusion provides a fast means of shuttling over large numbers of molecules at once, their size and number being limited only by the size of the enclosing bilayer compartment.

Membrane fusion can be defined as the process in which two lipid bilayer membranes come together, join at a molecular level, and merge. In many fusion events, two membrane-enclosed compartments coalesce, leading to mixing of the lipids in the membrane *via* lateral diffusion (Fig. 7). The fusing compartments can be separate or one compartment can be contained in the other. Alternatively, fusion occurs between two domains of a single membrane and leads to formation of two membrane-enclosed compartments (Fig. 7). The two membrane compartments formed during fusion can be either separate or one membrane compartment can be inside the other. 'Symmetric' or 'homotypic' fusion refers to fusion

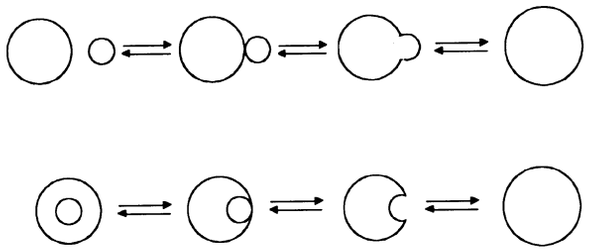

Fig. 7 Classification of all possible membrane fusion events. Membrane fusion can occur between two membrane-enclosed compartments which form one continuous membrane (left to right). Alternatively, one membrane can fuse with itself and form two separate membrane-enclosed compartments (right to left).

between membranes of identical composition. 'Asymmetric' or 'heterotypic' fusion is fusion between membranes having different compositions. Membrane fusion is a ubiquitous event in all eukaryotic cells and is a key feature of endocytosis, exocytosis, neurotransmission, intracellular transport, cell fusion, cytokinesis, viral infection, and many other cell biological processes. Both the molecular mechanism of biological membrane fusion and the intricate protein machinery that controls it continue to be a topic of intense biochemical interest. To summarise even the most recent results in this area is well beyond the scope of this review, and recent reviews on this topic are available.[24]

Briefly, we note that aggregation (*i.e.* close approach) of two bilayers is a prerequisite for membrane fusion. Since lipid bilayers repel each other due to a combination of repulsive electrostatic, hydration and entropic interactions,[54,55] aggregation is by no means a trivial condition for fusion. It is assumed that *in vivo* two bilayers are brought into close contact because anchoring proteins pull them together.[24] For bilayers containing anionic lipids, multivalent cations like calcium can be efficient fusogenic agents.[56,57] Calcium ions bind to the negatively charged phosphate moieties in the lipid head groups, reducing electrostatic repulsion, and removing large amounts of hydration water. In this way, binding of calcium ions induces local hydrophobic domains at the bilayer surface.[58,59] Furthermore, although at low calcium ion concentration '*cis*' (*intravesicular*) binding prevails, at sufficiently high concentrations of calcium ions '*trans*' (*intervesicular*) binding occurs, which leads to an additional bridging interaction between membranes, bringing them into molecular contact. Many other divalent and trivalent metal ions also induce aggregation of bilayers containing negatively charged lipids. Alternatively, bilayers can be brought into contact by polymer depletion interaction.[60,61]

Apart from bringing the bilayers together, effective fusogenic agents must induce local perturbations in the structure of the juxtaposed bilayers in order to permit the establishment of non-bilayer intermediate structures leading to membrane fusion. Proteins can cause local perturbations by insertion of a 'fusion peptide' into a target membrane and/or conformational changes upon insertion. Depending on the membrane lipid composition, calcium ions may induce domain formation[58,62,63] or phase transitions of the liquid crystalline bilayer to a gel-like lamellar state or an inverted hexagonal state,[56,64–66] both of which can result in local differences in lateral compressibility and packing defects. This makes the calcium ion unique compared to most other metal ions, which can induce bilayer aggregation, but not fusion. A local perturbation of the outer leaflets *must* be induced in order to trigger membrane fusion induced by poly(ethylene glycol).[60,61]

The views on the molecular rearrangements that must occur when two bilayer membranes merge into one have converged to an almost generally accepted model. The model is normally referred to as the modified stalk–pore theory of membrane fusion and has been proposed by Markin *et al.*[67] and further

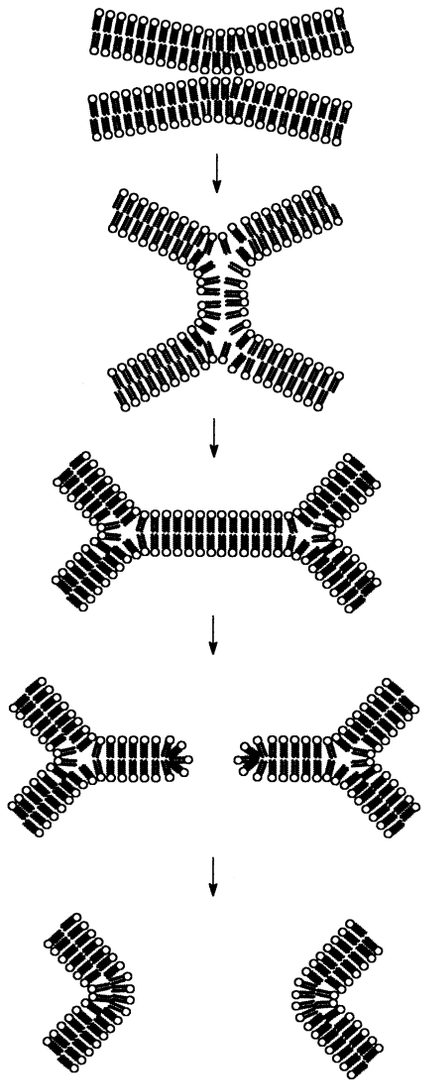

Fig. 8 Bilayer membrane fusion according to the stalk–pore model. Adjacent bilayers establish a contact site, a narrow stalk is formed, and the contact monolayers merge into a hemifusion diaphragm. Next, a pore is formed in the hemifusion diaphragm, and full fusion is achieved.

developed by Chernomordik[68,69] and Siegel.[70–72] The primary objective of the model (Fig. 8) is to provide a rearrangement of lipid molecules that allows for membrane fusion with minimal contact between the hydrophobic bilayer interior and the aqueous environment. According to the stalk–pore hypothesis, close approach of two bilayers is followed by the transient establishment of a stalk-like structure in which the adjacent (contact or '*cis*') membrane leaflets have merged, but the distal (non-adjacent or 'trans') leaflets remain intact. The driving force for stalk formation is strong van der Waals interaction between two adjacent bilayers. The Gibbs energy cost of stalk formation largely resides in the required bending of the membrane leaflets, and in the creation of hydrophobic voids at both ends of the stalk. Next, the stalk should expand into a hemifusion intermediate in which the two fusing compartments are separated by one mutual bilayer membrane, the '*trans* monolayer contact' (if it is small) or 'bilayer diaphragm' (if it is larger), consisting of the distal membrane leaflets of the fusing membranes. It is then proposed that either directly upon formation, or as the diaphragm widens, a minute hole forms in the diaphragm, leading to formation of a fusion pore of limited size. Pore formation is thought to be reversible up to a certain size, beyond which the pore irreversibly opens and full fusion is achieved (Fig. 8).

In sum, the modified stalk–pore model implies that bilayer membrane fusion is a cascade of sequential events. Stalk formation and hemifusion should result in mixing of lipid molecules in the *outer membrane leaflets* of fusing membranes. Fusion pore formation should be reversible, and should be accompanied by mixing of lipids in the *inner membrane leaflets* as well as the aqueous contents of the fusing membrane compartments. In addition, all stages of the fusion process should be extremely sensitive to modification of the spontaneous curvature of membrane leaflets (*vide infra*). This model of membrane fusion is supported by experimental evidence from a wide variety of bilayer membrane systems.[60,61,73]

The stalk–pore model of membrane fusion is based on considerations of hydrophobic attractions and curvature stress, but does not take into account electrostatic interactions and (de)hydration effects.[69,70] However, complexation of calcium ions to lipid head groups yields an essentially anhydrous calcium–lipid complex. Therefore, it is not certain that this model provides an accurate description of calcium-induced bilayer fusion. Calcium-induced fusion of small vesicles of phosphatidylserine has been described in terms of a so-called 'rupture–reseal' mechanism, in which the small vesicles initially fuse into large lamellar sheets, which roll up into multilamellar spiral lipid cylinders ('cochleate cylinders') that rearrange into large unilamellar vesicles only upon removal of calcium ions by EDTA.[74,75] Vesicles rapidly lose their contents in the course of these rearrangements. Calcium-induced fusion of vesicles of the synthetic lipid sodium di-*n*-dodecyl phosphate proceeds in a comparable way: small vesicles fuse into large flat vesicles, which rearrange into tubular calcium–lipid lamellar crystals.[76] However, for vesicles of many negatively charged lipids (including phosphatidylserine) and vesicles of mixtures of negatively charged and other lipids, there is ample evidence for the occurrence of non-leaky fusion of small vesicles into large vesicles.[77,78] The molecular rearrangements proposed for such 'tight' calcium-induced fusion processes are similar to the stalk–pore hypothesis.[57]

Although it has been tacitly assumed that a decreased propensity to fusion of polymerised bilayers in part explains their increased colloidal stability,[79] there are no systematic experimental studies of the fusion of vesicles of polymerised lipids. The work reviewed here is based on the hypothesis that when lipid mobility in the bilayer is restricted by means of covalent oligomerisation of the lipids, calcium-induced bilayer fusion will proceed more slowly and less efficiently. Calcium-induced vesicle aggregation of vesicles should not be affected by lipid oligomerisation. We carried out a systematic investigation of calcium-induced fusion of small unilamellar vesicles (50–100 nm) containing lipid oligomers either in both leaflets or exclusively in the inner membrane leaflet. It should be emphasised that the strict transmembrane asymmetry makes these vesicles fundamentally different from mixed liposomes of fusogenic and non-fusogenic lipids (such as phosphatidylserine and phosphatidylcholine[80–82] or phosphatidic acid and phosphatidylcholine[83]), which are known to fuse progressively more slowly as the phosphatidylcholine content is increased. Also, these vesicles are different from liposomes composed of membrane-spanning, 'bolaform' lipids, which are known to exhibit very slow fusion due to the fact that the membrane leaflets cannot diffuse independently.[84]

4.1 Calcium-induced fusion of vesicles of lipids with β-nitrostyrene head groups

The extent and the rate of lipid mixing during vesicle fusion were measured by the *n*-octadecyl rhodamine (R18) assay.[85] Under certain circumstances this assay disagrees with other fusion assays.[86] The resonance energy transfer (RET) assay employing rhodamine and NBD-labelled phosphatidylethanolamine[87] (NBD is 7-nitro-2,1,3-benzooxadiazole) or assays employing pyrene-labelled lipids[88] provided no suitable alternative since the BNS moiety inhibits efficient NBD or pyrene excitation, either through quenching or absorbance in the excitation wavelength range. However, the R18 and the RET assay yielded identical results for calcium-induced fusion of small vesicles of **5** (which does not interfere with NBD excitation), and therefore the R18 assay was employed with confidence. Moreover, in all experiments it was carefully verified that no probe exchange occurred spontaneously, and probe dilution was not observed in the absence of unlabelled vesicles.

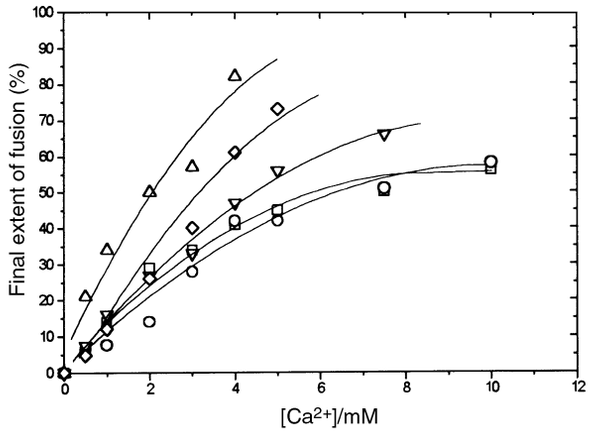

Fig. 9 Calcium ion concentration dependence of the extent of symmetric fusion of small vesicles of **1**–**5**; △, **1**; ◇, **2**; □, **3**; ○, **4**; ▽, **5**. Extents of fusion were recorded by the R18 assay for lipid mixing at 50 °C (60 °C for **4**).

An overview of the extent of fusion of small vesicles of BNS lipids (50–100 nm, prepared by sonication) as recorded by the R18 assay is presented in Fig. 9. All lipid vesicles fuse efficiently and rapidly. Small vesicles of lipids with short alkyl chains fuse more efficiently than small vesicles of lipids with longer alkyl chains (**1** > **2** > **3** > **4**). Hydrolysis of the BNS moiety has a marginal effect on the extent of fusion of small vesicles (compare **3** and **5**). No significant fusion occurs below the main phase transition temperature of the bilayers.

Vesicle fusion was examined in more detail for small vesicles of **3** at 50 °C. The extent of fusion was dependent on the calcium ion concentration: fusion is negligible below 0.5 mM of calcium ion, increases with calcium ion concentration up to 5 mM, and levels off at higher calcium ion concentrations. Fusion is strongly inhibited by oligomerisation of the lipids in the vesicles. No significant fusion occurs below 3 mM of calcium ion. Interestingly, inhibition is comparable for vesicles in which both membrane leaflets are oligomerised and vesicles in which only the inner membrane leaflet is oligomerised. The relative efficiency of inhibition is dependent on the calcium ion concentration: it is maximal up to 3 mM, and decreases at higher calcium concentrations. Similar observations were made for the rate of fusion. Fusion is fastest at the highest calcium concentrations, and is strongly retarded by oligomerisation of the bilayer. Retardation of fusion is more than 95% at low calcium ion concentration, and only slightly less at higher calcium ion concentrations. Furthermore, fusion proceeds more slowly in vesicles in which both membrane leaflets are oligomerised than in vesicles in which only the inner membrane leaflet is oligomerised. Comparable results were obtained for *large* vesicles of **3** and also for small vesicles of **1**.

The results from the lipid mixing assays were confirmed by TEM experiments with negatively-stained samples of vesicles of **1** and **3** prior to and after fusion (Fig. 10). The micrographs show the disappearance of most small vesicles and a large overall increase in vesicle diameter that occurs upon induction of fusion. In contrast, extensive aggregation, but no fusion is found for vesicles in which both membrane leaflets have been

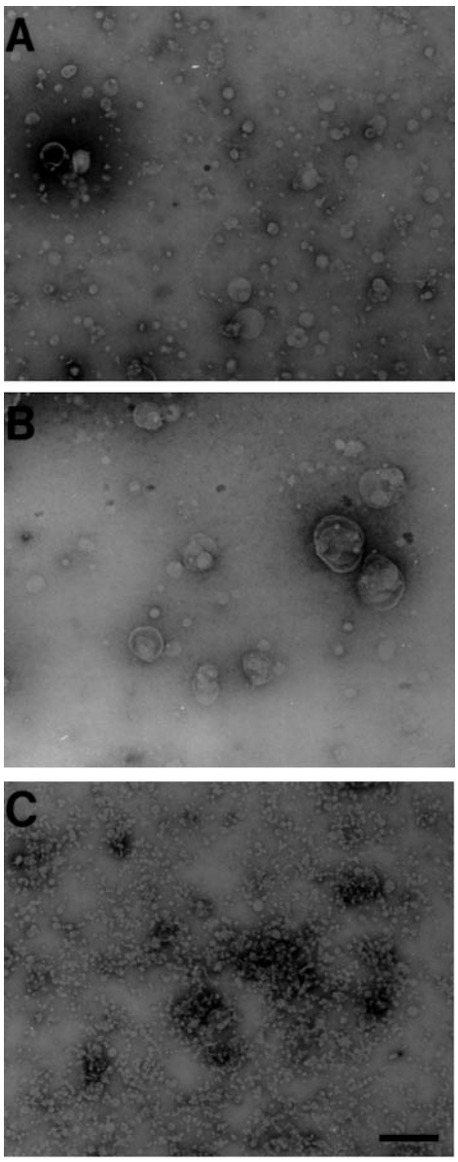

Fig. 10 Electron microscopy of vesicles of lipid **3**. (A) Small vesicles. (B) Large vesicles that result from the vesicles in (A) after addition of calcium chloride (5.0 mM), 2 min incubation at 50 °C, and quenching with EDTA. (C) Persistence of small vesicles of oligomerised lipid **3** after addition of calcium chloride at 50 °C. PTA (phosphotungstic acid) negatively-stained EM on formvar/carbon support. Scale bar represents 500 nm. (Reproduced by permission from *Biophys. J.* 1999, **76**, 374–386).

oligomerised. These findings were corroborated by QELS, which provided the average changes in vesicle diameter during the fusion process and confirmed the results of the R18 assays and TEM.

4.2 Asymmetric vesicle fusion

In addition to the symmetric vesicle fusion experiments, several asymmetric fusion experiments were monitored using the R18 assay. In these experiments, small vesicles of **3** were targeted at small vesicles of **4**, and *vice versa*. Since the experiments were carried out at 50 °C, vesicles of **4** have a gel-like bilayer ($T < T_m$) and no symmetric fusion can take place. Vesicles of **3** have a liquid-crystalline bilayer ($T > T_m$) and fusion occurs readily—both symmetrically and asymmetrically—but symmetric fusion is not reported by the assay, since it does not result in R18 dilution. Upon oligomerisation of the lipids in the vesicles of **3** (and *not* in the vesicles of **4**), lipid mixing is inhibited and retarded. Both inhibition and retardation are more pronounced when **3** is targeted at **4** than *vice versa*, and both are clearly less pronounced in the asymmetric experiments compared to the symmetric fusion experiments.

In a second set of asymmetric fusion experiments, vesicles of **1** were targeted at vesicles of **3**. In order to monitor both lipid mixing and contents leakage in the course of fusion, vesicles of **3** were either labelled with R18 or loaded with carboxyfluorescein (CF). The experiments were carried out at 25 °C, *i.e.* above T_m of **1**, but below T_m of **3**. Therefore, vesicles of **1** could fuse both symmetrically and asymmetrically, but vesicles of **3** could only fuse asymmetrically. According to the R18 assay, vesicles of **1** targeted at vesicles of **3** fuse efficiently. *No* significant leakage of CF is observed upon addition of calcium chloride, indicating an essentially non-leaky fusion process. However, CF is rapidly released *after addition of EDTA*, *i.e.* after quenching of the fusion process and after break-up of the aggregated clusters of fused vesicles. Hence, leakage during fusion is limited, but leakage is significant from the large, mixed vesicles of **1** and **3** that result from fusion. This conclusion is consistent with the finding that vesicles of **3** are impermeable to CF, whereas vesicles of **1** are leaky, and also with data indicating that calcium-induced liposome fusion can occur with retention of aqueous contents.[77,78] Also, CF leakage is secondary to lipid and contents mixing in calcium-induced fusion of phosphatidylserine liposomes.[89] When vesicles of oligomerised **1** were targeted at vesicles of oligomerised **3**, only minimal extents of lipid mixing and contents release were observed: the target vesicles retain their contents in the absence of fusion. Again, in all experiments the extent of lipid mixing and contents release increases with calcium ion concentration, but the inhibition due to oligomerisation decreases.

4.3 Fusion of oligomerised bilayer vesicles

Oligomerisation of lipid molecules does not influence calcium-induced vesicle aggregation, but strongly affects bilayer fusion of vesicles of the BNS lipids. Fusion is inhibited up to ten-fold in its extent, and fusion proceeds more than ten times more slowly. Lipid mixing and contents release assays, TEM and QELS yield consistent results. In all experiments, the inhibitions are less pronounced than the retardations. Lipid oligomerisation affects the kinetics rather than the extent of bilayer fusion. In absolute terms, lipid mixing during calcium-induced fusion of vesicles of BNS lipids occurs within 1–5 min, depending on temperature and calcium ion concentration. However, upon oligomerisation of the lipids, fusion proceeds much more slowly and takes up to 20 min to arrive at much lower final extents. Oligomerised lipid membranes *fuse in slow motion*. Inhibition and retardation of fusion are similar for vesicles in which only the inner membrane leaflet, or both the outer and the inner membrane leaflets are oligomerised. The additional inhibiting and/or retarding effect of oligomerisation of the lipids in the outer membrane leaflet is almost negligible. The composition of the inner rather than the outer membrane leaflet controls completion of bilayer fusion.[73]

It is important to appreciate that the inhibitions that are reported by the R18 assay are undoubtedly inhibitions of lipid mixing as a result of fusion, and not inhibitions of the *assay* as a result of slower lateral diffusion of the probe in the oligomerised membrane. Scrambling of lipid oligomers over the vesicle occurs on a time scale of seconds, whereas slow fusion requires up to 15 min.

The effect of lipid oligomerisation is dependent on three parameters. Firstly, the effect is more pronounced when more of the membranes participating are oligomerised, *e.g.* compare symmetric experiments (in which two oligomerised membranes fuse) and asymmetric experiments (in which only one of two fusing membranes is oligomerised). Secondly, the effect of oligomerisation decreases at higher calcium ion concentration. Presumably, more fusion contact sites can be established when more calcium ion is present, resulting in more rapid fusion. This

is consistent with the notion that calcium-induced liposome fusion is normally aggregation rate-limited, but becomes fusion rate-limited at high calcium ion concentration and reduced fusion rate.[89,90] Finally, the effect of lipid oligomerisation decreases with temperature. This is consistent with the concept of oligomerised lipids posing a kinetic barrier for fusion.

Membrane fusion is a localised event in which two adjacent membranes approach, establish a microscopic region of 'molecular contact', bend into sharply curved transient structures, and eventually merge into one continuous membrane. This process demands flexibility of the membrane, which is largely governed by the thermotropic state of the hydrocarbon interior, the lateral diffusion coefficient of the lipid molecules, and the spontaneous curvature of the membrane leaflets.

The propensity to fusion is low if not absent below the main phase transition temperature of the membrane.[91] In the gel-like lamellar state, the hydrocarbon interior has a rigid packing, lipids diffuse only slowly across and over the bilayer, and the membrane is stiff compared to the fluid state above T_m. However, according to the DSC data, the influence of lipid oligomerisation on the thermotropic phase behaviour of the hydrocarbon interior is modest, and cannot be invoked to explain the strong inhibition and retardation of fusion observed upon oligomerisation.

Rapid lateral diffusion of the lipid molecules in the membrane is a prerequisite for efficient membrane fusion. The molecular rearrangement of the lipid bilayers required in the course of fusion will only take place at an appreciable rate if the lipid molecules have a sufficient degree of freedom. Oligomerisation of the BNS lipid head groups results in a large reduction of the lipid lateral diffusion coefficient. If both the inner and the outer membrane leaflets are oligomerised, fusion is probably inhibited because the membrane will resist formation of membrane defects that might otherwise result in stalk-like fusion intermediates. If only the inner membrane leaflet is oligomerised, stalks may be formed but fusion pore formation is expected to be very slow. These considerations explain the strong inhibition and retardation of membrane fusion, even if the oligomerisation is induced in the inner membrane leaflet only. The observation that inhibition and retardation of fusion decrease with temperature is consistent with the notion of a decreased lateral diffusion of the oligomerised lipids: at higher temperatures, lateral diffusion is faster, and the effects of lipid oligomerisation diminish.

Concerning the spontaneous curvature of the bilayer, hemifusion is inhibited by lipids with a positive curvature (tending to form micelles) in the *outer* membrane leaflet, because they disfavour formation of stalk-like fusion sites with negative curvature.[73] In some cases, lipids with negative curvature (tending to form inverted phases) have a modest promoting effect.[73] In contrast, fusion pore formation and full fusion benefit from the presence of lipids with a positive curvature in the *inner* membrane leaflet, whereas lipids with a negative curvature have a strongly inhibiting effect.[73] The head groups of BNS lipids pack closer upon oligomerisation, which would promote increased negative curvature of the oligomerised membrane leaflet.[32,92] Thus, pore formation and full fusion would be inhibited if the inner membrane leaflet is oligomerised. This conclusion implies that hemifusion can occur, but full fusion is inhibited. The change of bilayer spontaneous curvature upon oligomerisation of the *outer* membrane leaflet may have only a small effect on membrane fusion.[73]

The role of calcium ions in the stages of the fusion process is not clear beyond the establishment of a region of molecular membrane contact. It is assumed that calcium-induced bilayer fusion is triggered by changes in lateral compressibility and structural defects that result from binding of calcium ions to negatively charged lipid head groups.[57] One could speculate that structural defects as well as phase transitions are kinetically suppressed in bilayers of oligomerised lipids, and that this suppression poses an additional barrier to calcium-induced fusion. Similarly, it is anticipated that structural defects and phase transitions occur more readily in bilayers of lipids with short hydrophobic chains than in bilayers of lipids with long hydrophobic chains, which may explain why the former fuse more readily.

5 Electron microscopic investigations of calcium-induced fusion of vesicles with an oligomerised inner membrane leaflet[21]

Structural characterisation of the lipid bilayer rearrangements in the course of membrane fusion is a long-standing challenge to electron microscopists. The main obstacle is the inherent transient and local nature of the fusion event. In addition, potential artefacts that arise during sample preparation frustrate electron microscopic studies. Staining, dehydration, vitrification, fracturing, and shear during blotting and film formation all pose risks to the fragile lipid structures that may occur during membrane fusion.[93] Our work using BNS lipids stems from the assumption that the oligomerisable lipid vesicles present a promising avenue towards structural characterisation of intermediate structures of membrane fusion. Bilayer vesicles of BNS lipids can be oligomerised exclusively in their inner leaflet, resulting in membranes with an extreme transverse asymmetry: while the outer leaflet is prone to fusion, the inner leaflet is not. The stalk–pore model of membrane fusion predicts that extensive hemifusion can occur between such bilayers, whereas full fusion will be strongly inhibited.[73]

Cryogenic transmission electron microscopy (c-TEM)[94] was chosen as a tool to examine the morphological changes of vesicles of lipids **1** and **3** in the course of calcium-induced fusion. In contrast to conventional TEM of negatively-stained samples, c-TEM is able to resolve the individual leaflets of bilayer vesicles. The experimental work reviewed here required a compromise between optimal conditions for c-TEM and limitations inherent in the model system of calcium-induced vesicle fusion. c-TEM would benefit from high lipid concentrations, large vesicle diameters (*ca.* 200 nm), and spherical symmetry, since in transmission view of a thin, vitrified film this would result in a neat coplanar arrangement of spheres in which interactions of adjacent bilayer membranes can be optimally resolved. On the other hand, selective *exo*-vesicular hydrolysis of the BNS lipids limits the lipid concentration (<2 mM). Moreover, it was found that **1** and **3** do not yield perfectly spherical vesicles under all conditions, and binding of calcium ions can lead to formation of very dense aggregates, which are not easily resolved by c-TEM.

5.1 Morphology and calcium-induced fusion of vesicles formed from lipid 3

Initially, several c-TEM experiments were carried out using formvar/carbon-coated grids as support for the vitrified sample solution. Addition of calcium chloride (2.5 mM) to sonicated vesicles with an oligomerised inner leaflet, incubated above T_m, resulted in the formation of small aggregates of vesicles (Fig. 11). The two leaflets composing the vesicle bilayer can clearly be discriminated as two separate lines separated by *ca.* 4 nm. Several of the aggregated vesicles share a common bilayer diaphragm. Possibly, this diaphragm is the result of *hemifusion* of these vesicles. We assume that the 'slow motion fusion' of the vesicles with an oligomerised inner leaflet increases the probability of vitrification of this intermediate stage of the fusion process. In several cases, the diaphragm extends over more than 20 nm. The diaphragms extending furthest show signs of rupture, indicating instability of the arrested bilayer conformation. We note that occasional superposition, instead of hemifusion, of two vesicles can also be observed (Fig. 11). Admittedly, the preparation of c-TEM samples on a formvar/carbon-coated support film may suffer from possible artefacts arising from absorption of the vesicles to the surface of the

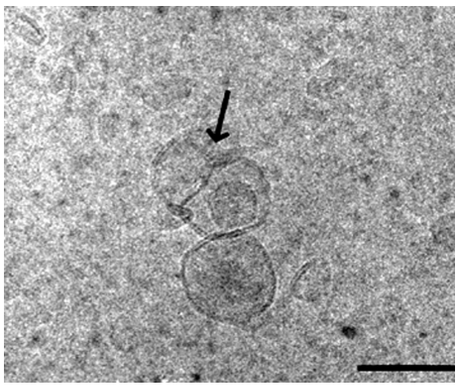

Fig. 11 Arrested hemifusion of vesicles of lipid **3** with an oligomerised inner bilayer leaflet. c-EM on formvar/carbon support. Scale bar represents 100 nm. (Reprinted from *Chem. Phys. Lipids*, **109**, *Electron microscopic investigation of the morphology and calcium-induced fusion of lipid vesicles with an oligomerised inner leaflet*, B. J. Ravoo, M. C. A. Stuart, A. D. R. Brisson, W. D. Weringa and J. B. F. N. Engberts, 63–74. Copyright 2001, with permission from Elsevier Science.)

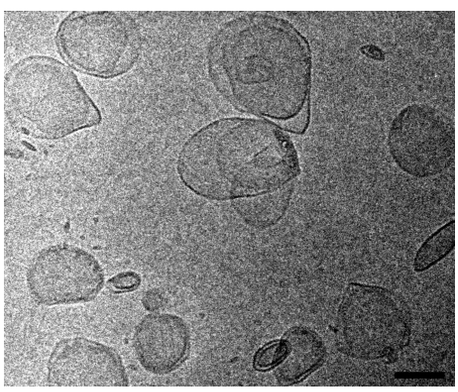

Fig. 12 Flattened and ellipsoidal vesicles of lipid **3** obtained after extrusion through 200 nm polycarbonate membranes. c-EM on holey carbon support. Scale bar represents 200 nm. (Reprinted from *Chem. Phys. Lipids*, **109**, *Electron microscopic investigation of the morphology and calcium-induced fusion of lipid vesicles with an oligomerised inner leaflet*, B. J. Ravoo, M. C. A. Stuart, A. D. R. Brisson, W. D. Weringa and J. B. F. N. Engberts, 63–74. Copyright 2001, with permission from Elsevier Science.)

support film. Therefore, Fig. 11 does not present unequivocal evidence of hemifusion of vesicles with an oligomerised inner leaflet.

Next, the samples were examined using vitrified aqueous films on holey carbon-coated copper grids in order to exclude the influence of surface adsorption of the aggregated vesicles. Under these experimental conditions, the bilayers could only be resolved as a single dark line. Surprisingly, control experiments showed that vesicles of **3** are flattened, ellipsoidal structures rather than spheres (Fig. 12). The morphology was not affected by the method of preparation of the vesicles (sonication, extrusion, dialysis), by the temperature of sample preparation, by the use of a Controlled Environment Vitrification System[95] for sample preparation, by oligomerisation of the inner leaflet, or by the ionic strength of the vesicle medium. The morphology is inherent to the molecular structure of **3**. This has also been observed for vesicles of several other synthetic lipids.[96,97] The atypical morphology of these vesicles can easily remain unnoticed in samples that are prepared on a formvar/carbon support, since vesicles tend to adsorb with their flattened side to the supporting film and appear spherical in projection (Fig. 10). Unfortunately, the irregular features of the flattened vesicles lead to an extremely complicated projection view. Aggregation and (hemi)fusion of such vesicles further increase the complexity, and it becomes difficult to discriminate between bilayer aggregation and (hemi)fusion, and to check the integrity of the bilayers.

5.2 Calcium-induced fusion of vesicles formed from lipid 1

Vesicles of lipid **1** display the anticipated smooth and spherical morphology when they are examined by c-TEM using a holey carbon-supported vitrified film of a sample solution. The bilayer is observed as a single dark line. As anticipated, the vesicles have a spherical morphology irrespective of their size and method of preparation, and the ionic strength of the aqueous medium. If vesicles are prepared by extrusion through a 200 nm polycarbonate membrane, so-called 'vase-like' vesicles with large invaginations are frequently encountered.[98,99]

Upon addition of calcium chloride (5 mM) to small or large vesicles of **1**, aggregates with diameters up to 300 nm are formed within 30 s. These aggregates have high density and a regular spacing of *ca.* 3 nm can be observed in the lipid packing. This spacing corresponds to the width of a dodecyl lipid bilayer, but it is too short for hydrated lipid bilayers at equilibrium distance, as in multilamellar vesicles. Possibly, the dense packing indicates almost completely dehydrated aggregates of calcium ions and **1**, as observed for phosphatidylserine[74] and for phosphatidylglycerol.[100] Upon addition of a four-fold excess of EDTA (relative to calcium ion) to the aggregates, they disperse within a few seconds and a solution of large unilamellar vesicles results. The formation of large aggregates upon calcium addition and the formation of large unilamellar vesicles upon EDTA addition are consistent with our QELS data.

It was observed that large vesicles of **1** (prepared by extrusion through a 200 nm polycarbonate membrane) show a morphological response to selective oligomerisation of the inner membrane leaflet: they lose their smooth spherical appearance and show invaginations as well as protrusions. Small vesicles (prepared by extrusion through a 100 nm membrane or by sonication) do not show such a morphological response. Possibly, the invaginations and protrusions are a consequence of the increased negative curvature of the inner leaflet as a result of oligomerisation of the head groups of the lipids in the inner leaflet. A similar curvature effect has been observed for other polymerisable lipids.[32,101] We assume that monolayer destabilisation as a result of curvature strain affects the morphology of bilayers of **1** but not of **3** because of the shorter hydrophobic chains that hold the bilayer together. Also, we assume that it affects large vesicles but not small ones, because small vesicles cannot respond due to inherent curvature restraints.

Upon addition of calcium chloride to small vesicles of **1** with an oligomerised inner leaflet, the formation of aggregates of *ca.* 100 nm diameter was observed. These aggregates are much smaller than those observed upon addition of calcium chloride to small vesicles of **1** without oligomerisation of the lipid head groups in the inner leaflet. Some aggregates contain only two or three vesicles. However, most aggregates were considerably larger and denser, showing closely packed multilayer rims. The aggregates become larger if either the calcium concentration or the incubation time is increased. The spacing of the rims is about 3 nm, as observed in the dense, calcium-induced aggregates of non-oligomerised vesicles. Upon addition of EDTA, the vesicles with an oligomerised inner leaflet behave very differently compared to the vesicles that are not oligomerised: the calcium-lipid aggregates disperse *slowly* into relatively small, *bilamellar* vesicles. In addition, networks of thread-like, branched unilamellar vesicles were observed that extend over several microns (Fig. 13). These rearrangements occur on a time scale of several min. The thread-like vesicles appear to grow from the aggregates. The width of the threads is variable, but no less than about 20 nm, as expected for two bilayers of charged lipids at equilibrium distance.

Thus, vesicles formed from lipid **1** fuse into dense aggregates upon addition of calcium chloride, but do so more slowly if they contain an oligomerised inner leaflet. In the latter case, fusing vesicles cannot be arrested in a hemifused intermediate

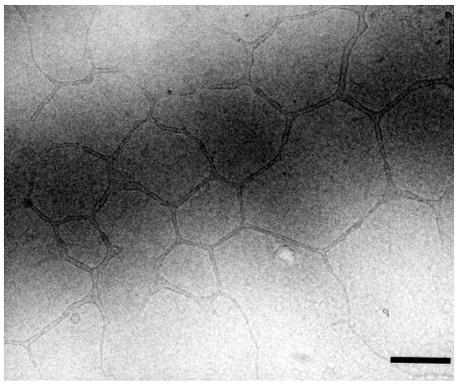

Fig. 13 Network of threads formed from vesicles of lipid **1** with an oligomerised inner bilayer leaflet incubated with calcium chloride (5.0 mM) for 30 s, then with EDTA (25 mM) for 30 s. c-EM on holey carbon support. Scale bar represents 200 nm. (Reprinted from *Chem. Phys. Lipids*, **109**, *Electron microscopic investigation of the morphology and calcium-induced fusion of lipid vesicles with an oligomerised inner leaflet*, B. J. Ravoo, M. C. A. Stuart, A. D. R. Brisson, W. D. Weringa and J. B. F. N. Engberts, 63–74. Copyright 2001, with permission from Elsevier Science.)

stage, as was occasionally observed in the case of vesicles of **3** with an oligomerised inner leaflet. It is likely that the stability of hemifusion intermediates decreases with decreasing hydrophobic chain length of the lipid molecules.[70]

On the other hand, vesicles formed from lipid **1** with an oligomerised inner leaflet fuse into multilamellar aggregates. The aggregates are dehydrated as a result of efficient binding of calcium ions to the head groups of **1**, which is reflected by the close packing of the lamellae. At present, whether or not the asymmetry of the fusing bilayers remains intact in the multilamellar arrangement is uncertain. The aggregates slowly disperse upon addition of EDTA, and one could imagine that a kinetic phase separation of lipid monomers and oligomers occurs at this stage, simply because the monomers will rearrange much faster than the oligomers. Perhaps the monomers end up in the bilamellar vesicles, whereas the oligomers build up the thread-like vesicles. The thread-like vesicle morphology could be the result of the preference of the linear lipid oligomers for a parallel orientation upon dispersal of the calcium-lipid aggregates. However, the mechanism of formation of the bilamellar vesicles is unclear. It is unlikely that the bilamellar vesicles are a result of shear-induced break-up of the network of thread-like vesicles, since this should produce unilamellar vesicles.

6 Thermodynamics of calcium-induced vesicle fusion[17]

A thermodynamic analysis of membrane fusion is a fundamental perspective that has remained underdeveloped both theoretically and experimentally. This is perhaps even more surprising in view of the extensive thermodynamic descriptions of shape transformations of bilayers.[102] The stalk–pore model of membrane fusion is partly based on calculations of the Gibbs energy of formation of hypothetical fusion intermediates from planar lipid bilayers.[70] Thus, the model provides some insight into the activation parameters of membrane fusion, albeit *in vacuo*, but it does not elucidate the thermodynamic driving force(s) of membrane fusion. The enthalpy of reaction between phosphatidylserine liposomes and calcium ions was measured[103] but the exothermic heat effect is a combined result of calcium–lipid binding, phase transitions in the bilayer, and liposome aggregation and fusion. A comparable exothermic effect was measured for the interaction between calcium ions and phosphatidylglycerol liposomes.[66] A microcalorimetric analysis of fusion between liposomes and Influenza virus indicated a rather strong endothermic enthalpy of membrane fusion.[22] Unfortunately, the thermodynamic analysis is complicated. Moreover, the authors confuse reaction enthalpies and Gibbs energies of activation, and do not elaborate on the potential entropic driving force for the endothermic process, and on the role of specific protein–lipid interactions. Simultaneously to the publication of our results,[17] a microcalorimetric analysis of proton-induced vesicle fusion was published.[23]

We determined the enthalpy of calcium-induced membrane fusion in a model system composed of vesicles of **1**, either in the absence or presence of a copolymer of lauryl methacrylate and acrylamide (LMPAM) that efficiently anchors into the hydrophobic interior of the bilayer.[104] In this model system, the complexities of the biological fusion event have been reduced to three, distinguishable processes: binding of calcium ion, vesicle aggregation, and bilayer fusion. Admittedly, this is a gross simplification of *in vivo* membrane fusion, but the results of this conceptually simple approach have general significance and provide insights into thermodynamics of calcium-induced membrane fusion.

6.1 Separating calcium ion binding, vesicle aggregation, and bilayer fusion

Small vesicles of lipid **1** fuse readily upon addition of calcium chloride at room temperature, but upon oligomerisation of the lipids, fusion is largely inhibited (*vide supra*). In the presence of a low concentration of LMPAM, no calcium-induced lipid mixing is observed at all. The minimal concentration of LMPAM required to completely inhibit lipid mixing corresponds to a molar ratio of **1** to LMPAM of 40 to 1. In contrast, poly(acrylamide) of comparable molecular weight does not affect fusion at these concentrations. The rate of aggregation of small vesicles prior to and after oligomerisation of **1** (measured as an increase in turbidity upon addition of calcium chloride) are equal. Whereas aggregation is not influenced by poly(acrylamide), no aggregation was observed if LMPAM was added to the vesicles in a lipid to polymer ratio of 40 to 1. Using TEM and QELS, it was found that in the absence of polymer, extensive vesicle fusion resulted in up to ten-fold increase in average vesicle diameter upon addition of calcium chloride. Similar observations were made in the presence of poly(acrylamide). However, fusion was blocked in the presence of LMPAM.

We contend that LMPAM provides the vesicles with a steric shield that prevents both aggregation and fusion, even at high concentrations of calcium ions. Similar observations have been described for liposomes containing a small percentage of poly(ethylene glycol)-derived lipids, as well as lipids substituted with various other water-soluble polymers.[10] Poly(acrylamide) has no hydrophobic moiety and is unable to anchor into the vesicle bilayer. Consequently, it lacks the inhibitory effect of LMPAM on aggregation and fusion. The polymer concentration is too low to induce fusion *via* depletion interaction.[60,61] In sum, lipid mixing assays, turbidity measurements and TEM, as well as QELS provide consistent evidence for a three-step calcium-induced fusion process of small vesicles of **1**, that can be stopped at any of the three successive stages. At room temperature, vesicles of **1** fuse efficiently. After oligomerisation of the lipid head groups in the vesicles, the vesicles bind calcium ion and aggregate, but they do not fuse. If the vesicles are coated with LMPAM, the vesicles bind calcium ions but do not aggregate or fuse.

6.2 Isothermal titration microcalorimetry and the thermodynamics of membrane fusion

In order to assess the thermodynamics of vesicle aggregation and bilayer fusion, titration experiments were carried out in an isothermal titration microcalorimeter. In the titration experiments, aliquots of a sonicated dispersion of small vesicles of **1** were injected into aqueous calcium chloride at 30 °C. The

Table 2 Enthalpies of calcium-induced aggregation and fusion of small vesicles of lipid **1**

Event[a]	Description	Enthalpy/kJ mol^{-1}
1	Calcium ion binding to vesicles of **1**, vesicle aggregation, bilayer fusion	9.74 ± 0.11
2	Calcium ion binding to vesicles of oligomerised **1**, vesicle aggregation	9.18 ± 0.10
3	Calcium ion binding to vesicles of **1**	6.96 ± 0.13
4	Calcium ion binding to vesicles of oligomerised **1**	6.55 ± 0.13
2 − 4	Vesicle aggregation	2.6 ± 0.1
(1 − 2) − (3 − 4)	Bilayer fusion	0.15 ± 0.1

[a] Numbering corresponds to Fig. 14.

traces of heat flow *vs.* time were integrated to obtain the corresponding enthalpies of reaction. Under these conditions, aggregation and fusion are rapid. As a result, each experiment yields an accurate reaction enthalpy, which was taken as the average for 10–12 injections.

The observed heat effect can be dissected into three well-defined processes: binding of calcium ion, aggregation of the vesicles, and the ultimate merging of the bilayers. In comparison, the thermodynamic analysis of virus-protein-induced membrane fusion is highly complicated.[22] The enthalpy accompanying the titration of vesicles of monomer lipid into the calcium chloride solution not only reflects aggregation and fusion, but also binding of calcium ion to the phosphate head groups, and any concomitant ion-dehydration effects. Similarly, titration of vesicles of oligomerised lipid into calcium chloride solution yields a reaction enthalpy that solely includes aggregation and binding of calcium ion to the phosphate head groups of the oligomerised lipids. However, binding of calcium ion to oligomerised and monomer lipid bilayers is not thermodynamically equivalent, and subtraction of the two heat effects does not yield the true enthalpy of vesicle fusion. This analytical problem was solved using the macromolecular hydrophobic anchor LMPAM, which allows for independent measurements of the effects of binding of calcium ion. In the presence of this polymer, aggregation and fusion are fully blocked for both oligomerised and monomer lipid and any differences in reaction enthalpies reflect differences in binding of calcium ion only. Applying this correction, the enthalpy of fusion can be calculated. The enthalpy of aggregation is obtained by subtracting the heat accompanying the titration of LMPAM-coated oligomerised vesicles into a calcium chloride solution (*binding only*) from the enthalpy for the titration of oligomerised vesicles into a calcium chloride solution of the same molarity (*aggregation* + *binding*). This approach is illustrated in Fig. 14, and Table 2 summarises the results.

The data show that binding of calcium ions to the phosphate head groups is endothermic by 7.0 kJ (mol **1**)$^{-1}$ before oligomerisation, and by 6.5 kJ (mol **1**)$^{-1}$ after oligomerisation. This enthalpy is lower than that accompanying binding of calcium ion to phosphate ion in aqueous solutions which is endothermic by 11.5–13 kJ mol^{-1}.[17] Calcium–phosphate binding is driven by the release of hydration water,[105] and the difference is accounted for by the fact that the phosphate head groups are less accessible to bind calcium ions at the vesicle surface, and that they are already partially dehydrated. It is likely that the binding of calcium ions to phosphate head groups of oligomerised **1** is slightly less endothermic than the binding to head groups of monomer **1**, because the oligomerised head groups are slightly dehydrated relative to the monomer head groups (as also indicated by DSC). Endothermic, entropy-driven binding of calcium ion to phosphatidylcholine/phosphatidylglycerol liposomes has been reported.[106]

Vesicle aggregation is endothermic by 2.6 ± 0.1 kJ (mol **1**)$^{-1}$ (Table 2). Vesicle aggregation is the result of endothermic but entropically favourable release of hydration water upon close approach of adjacent bilayers. Most likely, increased counterion binding of the lipid head groups contributes to this

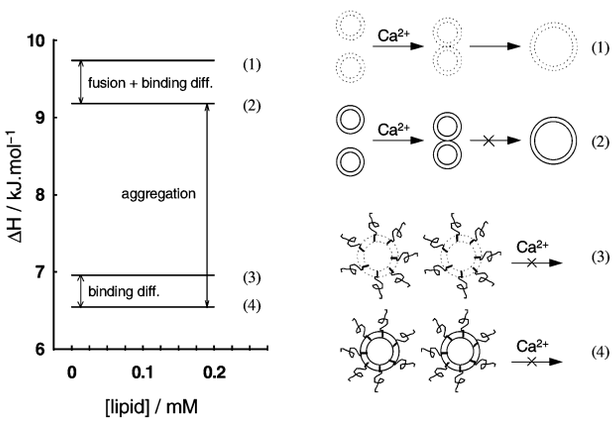

Fig. 14 Dissecting enthalpies of vesicle aggregation and bilayer fusion from calcium ion binding effects: a schematic representation. Monomer lipid bilayers are represented by dashed lines, oligomerised bilayers are represented by solid lines. Numbering corresponds to Table 2. (Reprinted with permission from *J. Phys. Chem. B*, 1998, **102**, 11001–11006. Copyright 1998 American Chemical Society.)

effect.[107] Since calcium-induced aggregation is a spontaneous process, the driving force is entropic.

Bilayer fusion is associated with a positive enthalpy of only 0.15 ± 0.1 kJ (mol **1**)$^{-1}$ (Table 2). Since the fusion of monomer lipid vesicles is not quantitative, and the inhibition of fusion upon oligomerisation is not complete, we put the value for *complete* vesicle fusion at 0.25 ± 0.10 kJ (mol **1**)$^{-1}$ rather than 0.15 ± 0.10 kJ (mol **1**)$^{-1}$. Reduction of bilayer curvature promotes formation of larger vesicles from small ones: vesicle fusion proceeds much more readily if the 'reactant' vesicle size remains below 100 nm.[108] Assuming that bilayer curvature becomes negligible, the Gibbs energy of fusion can be estimated as −225 kJ (mol vesicles)$^{-1}$,[109] *i.e.* approximately −0.0225 kJ (mol lipid)$^{-1}$ for bilayer vesicles of 10000 negatively charged lipids. Vesicle fusion is exergonic since it proceeds spontaneously upon addition of calcium chloride. Since bilayer fusion *per se* is associated with an endothermic enthalpy (we like to call this 'cold fusion'),[17] *entropy* should provide the driving force for fusion of bilayer membranes.

A key question is how the relief of curvature strain is expressed at the molecular level. The enthalpy associated with the gel to liquid-crystalline bilayer phase transition becomes more endothermic as the vesicle size increases, indicating a concomitant increase in lateral packing efficiency of lipid molecules.[110] There is further calorimetric evidence that relief of bilayer curvature is exothermic.[111] Also, bilayer compression is exothermic, and bilayer expansion is endothermic.[112] But if these were the dominant factors in vesicle fusion, formation of large vesicles from smaller ones would be enthalpically favourable. This is not consistent with the results that we and others obtained.[17,22,23] Most probably, the entropic driving force for fusion is provided by (1) the increase of the number of (translational, rotational, undulational) modes of freedom of the lipid molecules in going from aggregated clusters of small

vesicles to the conformationally less restricted, larger fusion products and (2) a release of hydration water from the lipid head groups as the bilayer curvature is relieved. Finally, the enthalpy loss upon fusion of pure lipid membranes is an order of magnitude smaller than that observed for proton-induced liposome fusion [1.7–2.5 kJ (mol lipid)$^{-1}$][23] as well as than that for protein-mediated virus–liposome fusion [2.5–3.0 kJ (mol viral lipid)$^{-1}$].[22] In both of these studies, lipids with hexadecyl and octadecyl hydrocarbon chains were used. It is possible that the enthalpic effects associated with rearrangements of these lipids required for membrane fusion are larger because of their increased hydrophobicity relative to **1**. Also, the enthalpy of mixing of protein-rich viral membrane and pure lipid membrane[113] could dominate the thermodynamics of fusion between virions and liposomes (*vide infra*).

7 Fusion of Sendai virus with vesicles of oligomerisable lipids[20]

Sendai virus or Hemagglutinating Virus from Japan (HVJ) is a paramyxovirus that infects cells by fusion with the cell membrane at neutral pH. The virus contains two different spike proteins that protrude from the viral envelope membrane: the HN glycoprotein (with two subunits of 15 and 51 kD) with hemagglutinating and neuramidase activity, and a second glycoprotein of 67 kD, also composed of two subunits.[114] One of the subunits of this second spike protein contains a distinct hydrophobic region at its amino terminal end.[115] The HN protein is involved in receptor-mediated binding to the cell surface, whereas the second protein mediates fusion with the target membrane. Therefore, the second spike protein is called the fusion or F protein. The physiologically relevant mode of action of Sendai requires a temperature of 37–40 °C and pH 7.4, and a target membrane of phosphatidylcholine and cholesterol that contains a sialic acid receptor (a ganglioside) to bind HN.[116–118] Fusion involves insertion of the hydrophobic amino terminus of one of the two subunits of the F protein into the target membrane.[119,120] Target membranes that contain negatively-charged lipids such as phosphatidylserine or cardiolipin (diphosphatidylglycerol) fuse more efficiently than membranes composed of neutral phospholipids.[118,121]

The crucial step in Sendai virus fusion is insertion of part of the F protein into the target membrane. Membrane insertion of the fusion peptide could have drastic influences on the thermodynamic characteristics of the fusion process.[113,122] Hydrophobic membrane binding of peptides is normally endothermic and driven by an entropically favourable release of hydration water.[123] However, several examples of 'non-classical' hydrophobic binding are known in which binding is enthalpy-driven, and the binding entropy is zero or even negative.[124–127] The thermodynamics of binding is strongly dependent on the internal lateral tension of the lipid membrane (the ease with which it permits insertion of foreign molecules), which is relatively low for small vesicles, and higher for membranes with less curvature (*i.e.* diameters exceeding 50 nm).[124]

We find that calcium-induced fusion of small vesicles is endothermic by 0.25 ± 0.10 kJ (mol lipid **1**)$^{-1}$. On the other hand, fusion of Influenza virus and liposomes is endothermic by 2.5–2.9 kJ (mol viral lipid)$^{-1}$.[22] Fusion between Influenza virus and liposomes occurs at pH 5.1 and involves insertion of a hydrophobic part of the Influenza hemagglutinin protein into the target membrane. Clearly, the heat effects in protein-mediated fusion are much larger than those observed in calcium-induced fusion of lipid vesicles. It was worthwhile to investigate whether the differences should be attributed to heat effects due to insertion of viral fusion proteins into the target vesicle membrane, due to lipid membrane fusion *per se*, or because of lipid–protein mixing as a result of fusion between the viral envelope and the target membrane. It has been shown that the contribution of viral and liposomal contents mixing is negligible.[22]

A related issue that required attention is the effect of buffer on the observed enthalpies of fusion, since in several calorimetric studies of peptide–lipid interactions a substantial buffer dependency has been found.[113,124,125,128] This buffer effect has been interpreted in terms of membrane binding-induced pK_a shifts of residues in the peptide that binds to or inserts into the membrane. Such pK_a shifts can either be the result of the transfer of charged α-amino acid residues from a polar to a hydrophobic environment, or (in the case of negatively-charged bilayers) arise from the fact that the local pH near a negatively-charged membrane is considerably lower than the pH in bulk solution, leading to protonation of residues upon transfer.[113] Depending on the α-amino acid composition of the peptide, the membrane binding-induced pK_a shift(s) may lead to either a net uptake or a net release of protons upon binding. These protons are absorbed or provided by the buffer medium, which causes a heat effect that is directly correlated to the ionisation enthalpy of the buffer. Therefore, common practice measures the heat effect of peptide–lipid interactions in several buffers of known ionisation enthalpy, and determines the *intrinsic heat effect* by extrapolation to zero buffer ionisation enthalpy. This consideration has been ignored in the calorimetric study of Influenza virus–liposome fusion, possibly due to the complicated analysis of such a buffer effect in a pH-dependent fusion process.[22] We have studied these effects in some detail.

7.1 Lipid mixing assays and TEM

Lipid mixing in the course of fusion between Sendai virus and small as well as large vesicles of **3** was monitored by the R18 assay. Fusion becomes faster and more extensive as the concentration of target membrane and/or the temperature are increased. Efficient fusion requires a large excess of target membrane. Sendai virus can fuse with vesicles of **3** *below* their main phase transition temperature. According to the R18 assay, fusion is strongly inhibited and retarded by oligomerisation of the lipid head groups. Inhibition and retardation of fusion diminish as the concentration of target membrane is increased, but even a 25-fold excess of target membrane oligomerisation still results in a 70–75% lower final extent and initial rate of fusion. TEM of samples of Sendai virus and vesicles of **3** confirmed the conclusions from the R18 fusion assays (Fig. 15). Moreover, the micrographs do not indicate aggregation of the virions and the oligomerised vesicles of **3**.

7.2 Isothermal titration microcalorimetry

The enthalpy of the interaction between Sendai virus and small vesicles of lipid **3** was measured using isothermal titration microcalorimetry. Aliquots of a suspension of Sendai virus were injected into the sample cell containing a solution of small vesicles of **3** at 37 °C. Upon each injection, endothermic heat effects were observed over a time scale of about one minute. The experiment was repeated in four different buffers of identical concentration and pH 7.40. The intensity of the observed heat effect was strongly dependent on the buffer medium (Table 3). As the ionisation enthalpy of the buffer increases, the reaction becomes more endothermic. A linear correlation relates the observed heat effect and the ionisation enthalpy of the buffer.[20] Extrapolation of the linear fit to zero buffer ionisation enthalpy yields an intrinsic heat effect for the interaction of Sendai virus with small vesicles of **3** of 4.3 ± 1.1 kJ (mol viral lipid)$^{-1}$. The positive slope of the plot of the observed heat effect *versus* the buffer ionisation enthalpy indicates that buffer dissociates during the interaction of Sendai virus and the vesicles, which implies an uptake of protons in the course of the fusion process. The slope is a quantitative measure for the number of protons that are taken up, and it amounts to 0.15 ± 0.04 mol protons (mol viral lipid)$^{-1}$.

Titrations of Sendai virus into small vesicles of *oligomerised* **3** yielded much smaller endothermic heat effects (Table 3).

Table 3 Heat effects accompanying titration of Sendai virus to vesicles of lipid **3** at 37 °C

Buffer	Buffer ionisation Enthalpy/kJ (mol buffer)$^{-1}$	Vesicles of **3** and Sendai Enthalpy/kJ (mol buffer)$^{-1}$	Vesicles of oligomerised **3** and Sendai Enthalpy/kJ (mol buffer)$^{-1}$
Phosphate	5.10	4.43 ± 0.58	2.55 ± 0.19
PIPES	12.4	5.90 ± 0.78	2.88 ± 0.18
HEPES	22.5	9.29 ± 1.0	2.68 ± 0.25
TRIS	48.1	11.2 ± 0.59	3.05 ± 0.46

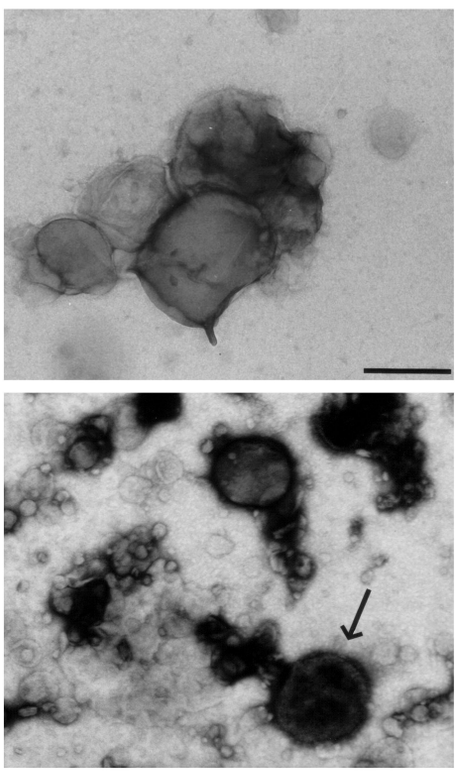

Fig. 15 Electron microscopy of mixtures of Sendai virus and small vesicles of lipid **3**. (A) Virus and vesicles incubated at 40 °C. (B) Virus and vesicles of oligomerised lipid **3** incubated at 40 °C. The arrow indicates an intact virion, easily identified because of its stained spike protein coating. Uranyl acetate negatively-stained EM on formvar support. Scale bar represents 200 nm. (Reproduced by permission from *Cell. Biol. Int.*, 2000, **24**, 787–797.)

Most interestingly, experiments in four different buffers yielded identical heat effects of 2.8 ± 0.2 kJ (mol viral lipid)$^{-1}$. This indicates that no protons are taken up (or released) during the interaction of Sendai virus with small vesicles of oligomerised **3**. Control experiments in which Sendai virus was titrated into phosphate and HEPES buffer solutions in the absence of vesicles revealed that the dilution of the concentrated virus suspension accounts for most of the heat effect that is observed in the titration of Sendai virus into oligomerised vesicles of **3**.

The buffer dependence of the heat effect observed upon fusion of Sendai virus with vesicles of **3** can in part be explained from the insertion of the F protein of Sendai virus into the target membrane. The only residue that contains a pH-sensitive group is the amino terminal α-phenylalanine, with a terminal NH_2 with a pK_a of *ca.* 8. This implies that the amino group is only partially protonated at pH 7.4. The microcalorimetric data, however, suggest that it is protonated, which is probably the result of the reduced local pH near the surface of the negatively-charged membrane (rather than deprotonated, which would imply a charge neutralisation that favours membrane insertion). Similar effects have been described in a calorimetric study of binding between a model peptide and liposomes.[124] However, it would be a gross oversimplification to suggest that only the residues in the amino terminal part of the F protein are affected during fusion with the target membrane. Certainly, in the course of the fusion event, a considerable part of the F protein as well as the HN protein will approach closely to the negatively-charged membrane. The F and HN proteins have their iso-electric point at pH 4.9 and pH 6.5, respectively,[114] which means that they are both negatively-charged at pH 7.4. Upon close association with the negatively-charged membrane (with low local pH), they will be protonated to some extent. Ultimately, fusion of Sendai virus with the target membrane results in merging of the viral envelope and the target bilayer membrane (as evidenced by the lipid mixing assay), implying a transfer of the viral spike proteins from a neutral to a negatively-charged membrane. Most certainly, the F and HN proteins will then be protonated to some extent. Unfortunately, these effects are difficult to quantify in terms of which α-amino acid residues are effected, and to what extent. The viral envelope contains about 100 lipid molecules per protein molecule.[129]

According to the plot of the observed heat effect against the buffer ionisation enthalpy, about 0.15 protons are taken up per viral lipid molecule, which means about 15 protons should be taken up per protein molecule. This may appear a large number, but both F and HN are composed of *ca.* 500 α-amino acids, many of which are potential proton acceptors.[115] Assuming an equimolar ratio of HN and F, it is obvious that protonation effects specifically related to insertion of the amino terminal part of the F protein (max. 0.5 proton per protein) are modest compared to protonation of F and HN as a result of membrane merging (almost 15 protons per protein).

The R18 assays of lipid mixing as well as TEM lead to the conclusion that fusion of Sendai virus with both small and large vesicles of **3** is inhibited by oligomerisation. Since no buffer dependence is observed for the heat effect of the titration of Sendai virus to vesicles of oligomerised **3**, it can be concluded that the F protein does not insert into or interact otherwise with this target membrane. Most likely, this is a direct consequence of the covalent linking of the lipid molecules as a result of the head group oligomerisation. Failure of the F protein to insert into the oligomerised vesicle membrane can explain the inhibition of fusion of Sendai virus with oligomerised vesicles of **3**. This conclusion is supported by TEM, which shows that Sendai virus and oligomerised vesicles of **3** do not aggregate.

Individual injections into the titration microcalorimeter can be compared to successive fusion experiments with a high ratio of target membrane to virus.[20] Therefore, the difference in the heat effect that is observed when comparing the titration of Sendai virus to vesicles of **3** prior to and after oligomerisation can be attributed to heat effects associated with the membrane fusion process that occurs between Sendai virus and the vesicles of **3**, and *not* with the oligomerised vesicles of **3**. The enthalpy of the fusion process is 4.3 ± 1.1 − 2.8 ± 0.2 kJ (mol viral lipid)$^{-1}$ = 1.5 ± 1.3 kJ (mol viral lipid)$^{-1}$. Hence, fusion is an endothermic process that requires an entropic driving force.

We observed a very small positive enthalpy for calcium-induced lipid bilayer merging amounting to *ca.* 0.25 kJ (mol lipid)$^{-1}$ for lipid **1**. Fusion of Sendai virus with vesicles of lipid **3** is endothermic by *ca.* 1.5 kJ (mol viral lipid)$^{-1}$. Therefore, fusion between vesicles and Sendai virus is an order of magnitude more endothermic than vesicle–vesicle fusion. However,

this comparison has to be made with considerable caution, since the thermodynamics of the fusion of vesicles of the dodecyl lipid could differ quantitatively from fusion of vesicles of the hexadecyl lipid, in spite of their close structural resemblance. We note that an enthalpy of 1.7–2.4 kJ (mol lipid)$^{-1}$ was found for proton-induced fusion of hexadecyl–octadecyl lipid vesicles.[23]

Nevertheless, it would be extremely informative if one could at least compare the enthalpy associated with these two fusion processes at a 'kJ per mol fusion events' basis. We attempted to do so in a qualitative manner. In order to translate the enthalpy of fusion per mole of lipid to the enthalpy per mole of fusion events, one needs to consider (1) the number of lipid molecules per vesicle and per virion and (2) the number of rounds of fusion that each vesicle (or virion) participates in. Since the Sendai virions are at least twice the size of the vesicles, the number of lipid molecules per virion is considerably higher than the number of lipids per vesicle. Therefore, the difference between the enthalpy of Sendai virus–vesicle fusion and the enthalpy of vesicle–vesicle fusion will be even greater when expressed per mole of virion (vesicle) instead of per mole of lipid. In the calcium-induced vesicle fusion experiments, about 10 small vesicles fused into 1 large vesicle, implying that the enthalpy reflects several rounds of fusion. Also in the course of fusion between Sendai virus and vesicles of **3**, each Sendai virion must participate in several rounds of fusion in order to achieve the extent of lipid mixing observed in the R18 assay, and the diameter of the fusion products observed by TEM. The vesicles of **3** are less than half the size of the Sendai virions, and an extent of fusion of 50 % corresponds to two-fold membrane probe dilution, implying fusion of one virion and four vesicles. Therefore, the enthalpy of Sendai virus–vesicle fusion represents a similar if not lower number of rounds of fusion as the enthalpy of vesicle–vesicle fusion. Thus, we assumed that the enthalpies reported here on a 'per mole lipid' basis also indicate a very significant difference on a 'per mole fusion events' basis: the enthalpy associated with Sendai virus–vesicle fusion is an order of magnitude larger than the enthalpy of vesicle–vesicle fusion.

This leads us to the conclusion that most of the enthalpy cost of Sendai virus–vesicle fusion is a result of merging of the viral envelope and the target membrane, rather than membrane fusion *per se*. We note that merging of the protein-rich viral envelope and the lipid bilayer formed from **3** could result in curvature strain, domain formation and phase transitions of viral lipids, or **3**, or both, accompanied by significant heat effects.[130,131] Most likely, **3** will undergo a gel-like to liquid crystalline phase transition upon transfer from the vesicles to the viral membrane, which could contribute to the observed endothermic enthalpy of fusion. Moreover, merging of the viral envelope with the vesicle bilayers is accompanied by protonation of some of the protein residues in the viral envelope proteins, which is expected to be an *exothermic* reaction. The overall enthalpy of this protonation is difficult to estimate, since we do not know which residues are involved, and to what extent they are protonated. In any case, the intrinsic enthalpy of the membrane merger must be even larger than 1.5 kJ (mol viral lipid)$^{-1}$, and, consequently, a strong entropic driving force is required. A significant entropy gain could result from the liberation of hydration water upon insertion of (part of) the F protein into the target membrane, as expected for a hydrophobic binding process. In addition, the thermodynamics of the fusion process may be interpreted in terms of the model proposed by Seelig,[124] which predicts that binding of the F protein and the target membrane is endothermic, because it requires enthalpy input to insert a protein into the target membrane. Provided a bilayer membrane is not exceedingly curved (the vesicle diameter should be 50 nm or more, which is the case here), the internal lateral tension in the membrane is high, and any gain in Van der Waals energy upon inserting a foreign hydrophobic molecule is overruled by the work required to make room for it. On the other hand, merging of a protein-rich and a protein-free membrane entails a large entropy gain because of a large increase in continuous membrane surface area, which results in an increased degree of freedom of the lipid and protein molecules.

8 Conclusions

In conclusion to this review, we briefly evaluate the results of the experimental work and estimate its contribution to a better understanding of bilayer membranes and membrane fusion. The use of a sophisticated membrane mimetic system has validated itself in the course of this study. The strength of the method rests in the structural (chemical) modifications of lipid components of the membrane, which can be used to steer the properties of the entire bilayer membrane in a predictable manner. Admittedly, the novel lipid molecules that contain a BNS moiety covalently linked to their phosphate head group are *synthetic* molecules. This fact alone may render the results less helpful in understanding natural phenomena in the critical eye of the biochemist or cell biologist. However, these lipid molecules are a versatile tool for obtaining kinetic, structural and thermodynamic data on the properties of bilayer membranes, and on bilayer membrane fusion in particular. All biological lipid bilayer membranes are transversely asymmetric, which can be understood from the fact that each side of the membrane faces a different environment. This study provided the first synthetic lipid bilayer with a comparable degree of functional asymmetry. Our model system provided membrane vesicles with outer membrane leaflets of lipid monomers, and inner membrane leaflets of oligomerised lipids. We contend that this asymmetry will inspire future studies. The lateral diffusion of lipid oligomers is much slower than the lateral diffusion of lipid monomers, and the lipid head groups pack closer after oligomerisation. In addition, membranes of oligomerised lipids are less permeable than membranes of lipid monomers.

The inhibiting effect of lipid oligomerisation on calcium-induced membrane fusion can be interpreted in terms of the stalk–pore model. Membrane leaflets composed of oligomerised lipids resist formation of local defects that would trigger calcium-induced fusion in membranes of monomer lipids. In cases where the inner leaflet is oligomerised, it is anticipated that fusion is retarded because pore formation is strongly inhibited. Many observations indicate that lipid oligomerisation poses a kinetic barrier to membrane fusion, rather than making it structurally impossible. If less oligomerised lipid is involved, if more fusogenic agent is applied, or if the temperature is raised, the inhibiting effect diminishes. One expects that a completely polymerised lipid membrane leaflet is not able to fuse under any circumstances.

Unfortunately, the electron microscopic investigations did not provide the unambiguous structural information that was hoped for. According to the stalk–pore model, asymmetric bilayer membranes with an oligomerised inner membrane leaflet should form lipid stalks and engage in hemifusion, but would not, or only very slowly, form pores in the hemifusion bilayer diaphragm (leading to complete fusion). Despite many attempts, we could not unambiguously prove that calcium-induced hemifusion of these membranes occurs. Experimental difficulties make the quest for bilayer fusion intermediates a demanding task and we cannot conclude that these fragile structures do not exist simply because they were not observed.

Furthermore, this work has led to significant progress in understanding the thermodynamic characteristics of membrane fusion. Isothermal titration microcalorimetry had not been applied equally successfully to this problem before, and our experimental results shed more light on the driving force for membrane fusion. Exploiting the oligomerisable lipids, and, in addition, coating the vesicles with a hydrophobically-modified

poly(acrylamide), it was possible to dissect calcium-induced vesicle fusion into successive steps of binding of calcium ion, aggregation of vesicles, and bilayer fusion. Isothermal titration calorimetry was used to determine the enthalpies associated with each of these processes, and it was possible to suggest a likely interpretation of the thermodynamic data. Binding of calcium ions to lipid head groups and aggregation of vesicles causes the bulk of the heat effect accompanying calcium-induced vesicle fusion. Fusion of bilayer membranes is slightly endothermic and driven by a gain in entropy. Dehydration of the lipid head groups dominates the enthalpy of vesicle fusion. Although the model system presents a gross simplification of biological fusion events, it serves as an illustration of the powerful combination of sophisticated membrane mimics and ultrasensitive microcalorimetry.

The latter approach was taken one step further in our study of the fusion of Sendai virus and vesicles of oligomerisable lipids. The viral membrane proteins mediate fusion between Sendai virus and vesicles. Fusion is strongly inhibited by lipid oligomerisation, most likely because the fusion peptide on the membrane protein of the virus cannot insert into the oligomerised lipid bilayer. Isothermal titration microcalorimetry shows that fusion of Sendai virus with these vesicles is endothermic, but most of the enthalpy cost resides in the insertion of the fusion protein into the vesicle membrane, and concomitant dehydration and protonation effects. As with calcium-induced vesicle fusion, fusion between Sendai virus and vesicles is entropy-driven. We suggest that all membrane fusion processes are driven by entropy.

9 References

1 (*a*) D. W. Deamer, E. Harang Mahon and G. Bosco, in *Nobel Symposium 84*, S. Bengtson, Ed., Columbia University Press, New York, 1994; (*b*) D. W. Deamer, *Microbiol. Mol. Biol. Rev.*, 1997, **62**, 239.
2 A. D. Bangham and R. W. Horne, *J. Mol. Biol.*, 1964, **8**, 660.
3 (*a*) R. R. C. New, Ed., *Liposomes: a practical approach*, Oxford University Press, Oxford, 1990; (*b*) D. D. Lasic, *Liposomes: from physics to applications*, Elsevier, Amsterdam, 1993.
4 T. Kunitake and Y. Okahata, *J. Am. Chem. Soc.*, 1977, **99**, 3860.
5 J. H. Fendler, *Membrane mimetic chemistry*, Wiley, New York, 1982.
6 T. Kunitake, *Angew. Chem., Int. Ed. Engl.*, 1992, **31**, 709.
7 J. B. F. N. Engberts and D. Hoekstra, *Biochim. Biophys. Acta*, 1995, **1241**, 323.
8 F. M. Menger and K. D. Gabrielson, *Angew. Chem., Int. Ed. Engl.*, 1995, **34**, 2091.
9 P. L. Luisi and P. Walde, Eds., *Giant vesicles*, Wiley, Chichester, 2000.
10 D. D. Lasic, *Angew. Chem., Int. Ed. Engl.*, 1994, **33**, 1685.
11 (*a*) J. E. Rothman and J. Lenard, *Science*, 1977, **195**, 743; (*b*) J. A. F. op den Kamp, *Ann. Rev. Biochem.*, 1979, **48**, 47.
12 R. B. Gennis, *Biomembranes: molecular structure and function*, Springer Verlag, New York, 1989.
13 (*a*) R. A. Moss and S. Swarup, *J. Am. Chem. Soc.*, 1986, **108**, 5341; (*b*) R. A. Moss, S. Bhattacharya, P. Scrimin and S. Swarup, *J. Am. Chem. Soc.*, 1987, **109**, 5740; (*c*) R. A. Moss, S. Bhattacharya and S. Chatterjee, *J. Am. Chem. Soc.*, 1989, **111**, 3680; (*d*) R. A. Moss and S. Bhattacharya, *J. Am. Chem. Soc.*, 1995, **117**, 8688; (*e*) R. A. Moss, B. D. Park, P. Scrimin and G. Ghirlanda, *J. Chem. Soc., Chem. Commun.*, 1995, 1627.
14 H. Ringsdorf and B. Schlarb, *Makromol. Chem.*, 1988, **189**, 299.
15 H. Ringsdorf, B. Schlarb and J. Venzmer, *Angew. Chem., Int. Ed. Engl.*, 1988, **27**, 113.
16 B. J. Ravoo, W. D. Weringa and J. B. F. N. Engberts, *Langmuir*, 1996, **12**, 5773.
17 B. J. Ravoo, J. Kevelam, W. D. Weringa and J. B. F. N. Engberts, *J. Phys. Chem. B.*, 1998, **102**, 11001.
18 B. J. Ravoo, PhD Thesis, University of Groningen, 1998.
19 B. J. Ravoo, W. D. Weringa and J. B. F. N. Engberts, *Biophys. J.*, 1999, **76**, 374.
20 B. J. Ravoo, W. D. Weringa and J. B. F. N. Engberts, *Cell Biol. Int.*, 2000, **24**, 787.
21 B. J. Ravoo, M. C. A. Stuart, A. D. R. Brisson, W. D. Weringa and J. B. F. N. Engberts, *Chem. Phys. Lipids*, 2001, **109**, 63.
22 S. Nebel, I. Bartoldus and T. Stegmann, *Biochemistry*, 1995, **34**, 5705.
23 M. R. Wenk and J. Seelig, *Biochim. Biophys. Acta*, 1998, **1372**, 227.
24 (*a*) J. E. Rothman, *Protein Sci.*, 1996, **5**, 185; (*b*) P. G. Woodman, *Biochim. Biophys. Acta*, 1997, **1357**, 155; (*c*) J. E. Gerst, *Cell. Mol. Life Sci.*, 1999, **55**, 707.
25 (*a*) D. B. Miller, PhD Thesis, Ohio State University, 1957, (*Diss. Abstr.*, 1958, **18**, 1981); (*b*) A. V. Topchiev and V. P. Alaniya, *J. Polym. Sci. A*, 1963, **1**, 599.
26 R. Stewart, *J. Am. Chem. Soc.*, 1952, **74**, 4531.
27 (*a*) M. J. Blandamer, B. Briggs, P. M. Cullis, J. A. Green, M. Waters, G. Soldi, J. B. F. N. Engberts and D. Hoekstra, *J. Chem. Soc., Faraday Trans.*, 1992, **88**, 3431; (*b*) M. J. Blandamer, B. Briggs, P. M. Cullis, J. B. F. N. Engberts and D. Hoekstra, *J. Chem. Soc., Faraday Trans.*, 1994, **90**, 1905.
28 G. Cevc, Ed., *Phospholipids Handbook*, Marcel Dekker, New York, 1993.
29 R. Homan and H. J. Powell, *Biochim. Biophys. Acta*, 1988, **938**, 155.
30 R. A. Moss, *Pure Appl. Chem.*, 1994, **66**, 851.
31 W. Reed, L. Guterman, P. Tundo and J. H. Fendler, *J. Am. Chem. Soc.*, 1984, **106**, 1897.
32 H. Meier, I. Sprenger, M. Bärmann and E. Sackmann, *Macromolecules*, 1994, **27**, 7581.
33 See ref. 24a for a sunny account of the dimerisation of *p*-hydroxy-β-nitrostyrene on the roof of the Department of Chemistry at Ohio State University.
34 Y. Matsushita, E. Hasegawa, K. Eshima, H. Ohno and E. Tsuchida, *Makromol. Chem., Rapid Commun.*, 1987, **8**, 1.
35 A. Singh and J. M. Schnur, in *Phospholipids Handbook*, G. Cevc, Ed., Marcel Dekker, New York, 1993, pp. 233–291.
36 T. D. Sells and D. F. O'Brien, *Macromolecules*, 1994, **27**, 226.
37 H. Lamparski and D. F. O'Brien, *Macromolecules*, 1995, **28**, 1786.
38 S. L. Regen, B. Czech and A. Singh, *J. Am. Chem. Soc.*, 1980, **102**, 6638.
39 H. Hub, B. Hupfer, H. Koch and H. Ringsdorf, *Angew. Chem., Int. Ed. Engl.*, 1980, **19**, 938.
40 S. L. Regen, J. Shin and K. Yamaguchi, *J. Am. Chem. Soc.*, 1984, **106**, 2446.
41 H. Ringsdorf, B. Schlarb, P. N. Tyminski and D. F. O'Brien, *Macromolecules*, 1988, **21**, 671.
42 J. Lei and D. F. O'Brien, *Macromolecules*, 1994, **27**, 1381.
43 (*a*) D. E. Bennett and D. F. O'Brien, *J. Am. Chem. Soc.*, 1994, **116**, 7933; (*b*) D. E. Bennett and D. F. O'Brien, *Biochemistry*, 1995, **34**, 3102.
44 J. M. Park, S. Aoyama, W. Zhang, Y. Nakatsuji and I. Ikeda, *Chem. Commun.*, 2000, 231.
45 A. Blume, *Chem. Phys. Lipids*, 1991, **57**, 253.
46 K. Hirano, H. Fukuda and S. L. Regen, *Langmuir*, 1991, **7**, 1045.
47 A. Kusumi, M. Singh, D. A. Tirrell, G. Oehme, A. Singh, N. K. P. Samuel, J. S. Hyde and S. L. Regen, *J. Am. Chem. Soc.*, 1983, **105**, 2975.
48 (*a*) R. C. MacDonald and S. A. Simon, *Proc. Natl. Acad. Sci. USA*, 1987, **84**, 4089; (*b*) H. Möhwald, in *Phospholipid Handbook*, G. Cevc, Ed., Marcel Dekker, New York, 1993, pp. 579–602.
49 H. Ringsdorf, G. Schmidt and J. Schneider, *Thin Solid Films*, 1987, **152**, 207.
50 (*a*) P. R. Cullis, *FEBS Lett.*, 1976, **70**, 223; (*b*) E. E. Burnell, P. R. Cullis and B. de Kruiff, *Biochim. Biophys. Acta*, 1980, **603**, 63.
51 R. Ebelhäuser and H. W. Spiess, *Ber. Bunsenges. Phys. Chem.*, 1985, **89**, 1208.
52 A. C. McLaughlin, P. R. Cullis, J. A. Berden and R. E. Richards, *J. Magn. Reson.*, 1975, **20**, 146.
53 U. Kragh-Hansen, M. le Maire, J. P. Noël, T. Gulik-Krzywicki and J. V. Møller, *Biochemistry*, 1993, **32**, 1648.
54 J. N. Israelachvili, *Intermolecular surface forces*, Academic Press, New York, 1992.
55 J. N. Israelachvili and H. Wennerström, *Nature*, 1996, **379**, 219.
56 D. Papahadjopoulos, *Cell Surf. Rev.*, 1978, **5**, 765.
57 D. Papahadjopoulos, S. Nir and N. Düzgünez, *J. Bioenerg. Biomembr.*, 1990, **22**, 157.
58 S. Ohki, *Biochim. Biophys. Acta*, 1982, **689**, 1.
59 D. E. Leckband, C. A. Helm and J. Israelachvili, *Biochemistry*, 1993, **32**, 1127.
60 J. Lee and B. R. Lentz, *Biochemistry*, 1997, **36**, 6251.
61 B. R. Lentz and J. K. Lee, *Mol. Membr. Biol.*, 1999, **16**, 279.
62 D. M. Haverstick and M. Glaser, *Proc. Natl. Acad. Sci. USA*, 1987, **84**, 4475.
63 P. Garidel and A. Blume, *Langmuir*, 2000, **16**, 1662.
64 P. R. Cullis and B. de Kruijff, *Biochim. Biophys. Acta*, 1979, **559**, 399.
65 K. Hong, P. A. Baldwin, T. M. Allen and D. Papahadjopoulos, *Biochemistry*, 1988, **27**, 3947.
66 P. Garidel and A. Blume, *Langmuir*, 1999, **15**, 5526.

67 V. S. Markin, M. M. Kozlov and V. L. Borovjagin, *Gen. Physiol. Biophys.*, 1984, **5**, 361.
68 L. V. Chernomordik, G. B. Melikyan and Y. A. Chizmadzhev, *Biochim. Biophys. Acta*, 1987, **906**, 309.
69 L. V. Chernomordik and J. Zimmerberg, *Curr. Opin. Struct. Biol.*, 1995, **5**, 541.
70 D. P. Siegel, *Biophys. J.*, 1993, **65**, 2124.
71 D. P. Siegel and R. M. Epand, *Biophys. J.*, 1997, **73**, 3089.
72 D. P. Siegel, *Biophys. J.*, 1999, **76**, 291.
73 (*a*) C. Nanavati, V. S. Markin, A. F. Oberhauser and J. M. Fernandez, *Biophys. J.*, 1992, **63**, 1118; (*b*) L. V. Chernomordik, S. S. Vogel, A. Sokoloff, H. O. Onaran, E. A. Leikina and J. Zimmerberg, *FEBS Lett.*, 1993, **318**, 71; (*c*) A. Walter, P. L. Yeagle and D. P. Siegel, *Biophys. J.*, 1994, **66**, 366; (*d*) L. V. Chernomordik, A. Chanturiya, J. Green and J. Zimmerberg, *Biophys. J.*, 1995, **69**, 922; (*e*) L. V. Chernomordik, M. M. Kozlov and J. Zimmerberg, *J. Membr. Biol.*, 1995, **146**, 1; (*f*) G. B. Melikyan, S. A. Brener, D. C. Ok and F. S. Cohen, *J. Cell Biol.*, 1997, **136**, 995; (*g*) A. Chanturiya, L. V. Chernomordik and J. Zimmerberg, *Proc. Natl. Acad. Sci. USA*, 1997, **94**, 14423; (*h*) D. P. Pantazatos and R. C. MacDonald, *J. Membr. Biol.*, 1999, **170**, 27; (*i*) P. Meers, S. Ali, R. Erukulla and A. S. Janoff, *Biochim. Biophys. Acta*, 2000, **1467**, 227.
74 D. Papahadjopoulos, W. J. Vail, K. Jacobson and G. Poste, *Biochim. Biophys. Acta*, 1975, **394**, 483.
75 B. Kachar, N. Fuller and R. P. Rand, *Biophys. J.*, 1986, **50**, 779.
76 (*a*) L. A. M. Rupert, J. F. L. van Breemen, E. F. J. van Bruggen, J. B. F. N. Engberts and D. Hoekstra, *J. Membr. Biol.*, 1987, **95**, 255; (*b*) L. Streefland, F. Yuan, P. Rand, D. Hoekstra and J. B. F. N. Engberts, *Langmuir*, 1992, **8**, 1715; (*c*) T. A. A. Fonteijn, D. Hoekstra and J. B. F. N. Engberts, *Langmuir*, 1992, **8**, 2437.
77 J. Wilschut, N. Düzgünez, K. Hong, D. Hoekstra and D. Papahadjopoulos, *Biophys. Biochim. Acta*, 1983, **734**, 309.
78 S. W. Hui, S. Nir, T. P. Stewart, L. T. Boni and S. K. Huang, *Biochim. Biophys. Acta*, 1988, **941**, 130.
79 J. H. Fendler, *Science*, 1984, **223**, 890.
80 N. Düzgünez, J. Wilschut, R. Fraley and D. Papahadjopoulos, *Biochim. Biophys. Acta*, 1981, **642**, 182.
81 N. Düzgünez, S. Nir, J. Wilschut, J. Bentz, C. Newton, A. Portis and D. Papahadjopoulos, *J. Membr. Biol.*, 1981, **59**, 115–125.
82 J. R. Silvius and J. Gagné, *Biochemistry*, 1984, **23**, 3241.
83 R. Leventis, J. Gagné, N. Fuller, R. P. Rand and J. R. Silvius, *Biochemistry*, 1986, **25**, 6978.
84 (*a*) A. Relini, D. Cassinadri, Q. Fan, A. Gulik, Z. Mirghani, M. de Rosa and A. Gliozzi, *Biophys. J.*, 1996, **71**, 1789; (*b*) M. G. L. Elferink, J. F. L. van Breemen, W. N. Konings, A. J. M. Driessen and J. Wilschut, *Chem. Phys. Lipids*, 1997, **88**, 37.
85 D. Hoekstra, T. de Boer, K. Klappe and J. Wilschut, *Biochemistry*, 1984, **23**, 5675.
86 (*a*) T. Stegmann, P. Schoen, R. Bron, J. Wey, I. Bartoldus, A. Ortiz, J. L. Nieva and J. Wilschut, *Biochemistry*, 1993, **32**, 11330; (*b*) T. Stegmann, J. G. Orsel, J. D. Jamieson and P. J. Padfield, *Biochem. J.*, 1995, **307**, 875.
87 D. K. Struck, D. Hoekstra and R. E. Pagano, *Biochemistry*, 1981, **20**, 4093.
88 Y. Pal, Y. Barenholz and P. R. Wagner, *Biochemistry*, 1988, **27**, 30.
89 J. Wilschut, N. Düzgünez, R. Fraley and D. Papahadjopoulos, *Biochemistry*, 1980, **19**, 6011.
90 S. Nir, J. Bentz and J. Wilschut, *Biochemistry*, 1980, **19**, 6030.
91 J. Wilschut, N. Düzgünez, D. Hoekstra and D. Papahadjopoulos, *Biochemistry*, 1985, **24**, 8.
92 E. Sackmann, H. P. Duwe and H. Engelhardt, *Faraday Discuss. Chem. Soc.*, 1986, **81**, 281.
93 K. N. J. Burger, L. J. Calder, P. M. Frederik and A. J. Verkleij, *Methods Enzymol.*, 1993, **220**, 362.
94 M. Almgren, K. Edwards and G. Karlsson, *Colloids Surf., A*, 2000, **174**, 3.
95 J. R. Bellare, H. T. Davis, L. E. Scriven and Y. Talmon, *J. Electron Microsc. Tech.*, 1988, **10**, 87.
96 L. Hammarström, I. Velikian, G. Karlsson and K. Edwards, *Langmuir*, 1995, **11**, 408.
97 H. F. Zirkzee, Ph. D. Thesis, Technical University of Eindhoven, 1997.
98 D. D. Lasic, H. Strey, M. C. A. Stuart, R. Podgornik and P. M. Frederik, *J. Am. Chem. Soc.*, 1997, **119**, 832.
99 D. H. W. Hubert, M. Jung, P. M. Frederik, P. H. H. Bomans, J. Meuldijk and A. L. German, *Langmuir*, 2000, **16**, 8973.
100 P. Garidel, G. Förster, W. Richter, B. H. Kunst, G. Rapp and A. Blume, *Phys. Chem. Chem. Phys.*, 2000, **2**, 4537.
101 M. Jung, I. Den Ouden, A. Montoya-Goñi, D. H. W. Hubert, P. M. Frederik, A. M. van Herk and A. L. German, *Langmuir*, 2000, **16**, 4185.
102 R. Lipowsky, *Nature*, 1991, **349**, 475.
103 S. J. Rehfeld, N. Düzgünez, C. Newton, D. Papahadjopoulos and D. J. Eatough, *FEBS Lett.*, 1981, **123**, 249.
104 (*a*) J. Kevelam, J. F. L. van Breemen, W. Blokzijl and J. B. F. N. Engberts, *Langmuir*, 1996, **12**, 4709; (*b*) J. Simon, M. Kühner, H. Ringsdorf and E. Sackmann, *Chem. Phys. Lipids*, 1995, **76**, 241; (*c*) H. Ringsdorf, E. Sackmann, J. Simon and F. M. Winnik, *Biochim. Biophys. Acta*, 1993, **1153**, 335.
105 R. R. Irani and C. F. Callis, *J. Phys. Chem.*, 1960, **64**, 1398.
106 R. Lehrmann and J. Seelig, *Biochim. Biophys. Acta*, 1994, **1189**, 89.
107 J. Bentz and H. Ellens, *Colloids Surf.*, 1988, **30**, 65.
108 S. Nir, J. Wilschut and J. Bentz, *Biochim. Biophys. Acta*, 1982, **688**, 275.
109 M. Bergström and J. C. Eriksson, *Langmuir*, 1996, **12**, 624.
110 B. Grünewald, S. Stankowski and A. Blume, *FEBS Lett.*, 1979, **102**, 227.
111 R. M. Epand and R. F. Epand, *Biophys. J.*, 1994, **66**, 1450.
112 S. Nebel, P. Ganz and J. Seelig, *Biochemistry*, 1997, **36**, 2853.
113 J. Seelig, *Biochim. Biophys. Acta*, 1997, **1331**, 103.
114 K. Shimizu, Y. K. Shimizu, T. Kohama and N. Ishida, *Virology*, 1974, **62**, 90.
115 M. J. Gething, J. M. White and M. D. Waterfield, *Proc. Natl. Acad. Sci. USA*, 1978, **75**, 2737.
116 A. M. Haywood and B. P. Boyer, *Biochemistry*, 1982, **21**, 6041.
117 V. Citovsky, R. Blumenthal and A. Loyter, *FEBS Lett.*, 1985, **193**, 135.
118 K. Klappe, J. Wilschut, S. Nir and D. Hoekstra, *Biochemistry*, 1986, **25**, 8252.
119 M. Hsu, M. Scheid and P. W. Choppin, *J. Biol. Chem.*, 1981, **256**, 3557.
120 S. L. Novick and D. Hoekstra, *Proc. Natl. Acad. Sci. USA*, 1988, **85**, 7433.
121 A. M. Haywood and B. P. Boyer, *Biochemistry*, 1984, **23**, 4161.
122 M. R. Wenk and J. Seelig, *Biochemistry*, 1998, **37**, 3909.
123 C. J. Russel, T. E. Thorgeirsson and Y. Shin, *Biochemistry*, 1996, **35**, 9526.
124 G. Beschiaschvili and J. Seelig, *Biochemistry*, 1992, **31**, 10044.
125 J. Seelig, S. Nebel, P. Ganz and C. Bruns, *Biochemistry*, 1993, **32**, 9714.
126 P. G. Thomas and J. Seelig, *Biochem. J.*, 1993, **291**, 397.
127 (*a*) D. B. Smithrud, T. B. Wyman and F. Diederich, *J. Am. Chem. Soc.*, 1991, **113**, 5420; (*b*) B. R. Peterson, P. Walliman, D. R. Carcanaque and F. Diederich, *Tetrahedron*, 1995, **51**, 401.
128 B. M. Baker and K. P. Murphy, *Biophys J.*, 1996, **71**, 2049.
129 A. Loyter and D. J. Volsky, *Cell Surf. Rev.*, 1982, **8**, 215.
130 R. M. Epand, *Biochim. Biophys. Acta*, 1998, **1376**, 353.
131 T. Gil, J. H. Ipsen, O. G. Mouritsen, M. C. Sabra, M. M. Sperotto and M. J. Suckermann, *Biochim. Biophys. Acta*, 1998, **1376**, 245.